

SEPARATION CRITERIA OF A NONLINEAR CONTACT  
SYSTEM, IN A STEADY STATE SINUSOIDAL  
VIBRATION ENVIRONMENT

By

MORRIS CHARLES BURKHART

Bachelor of Science  
Oklahoma State University  
Stillwater, Oklahoma  
1962

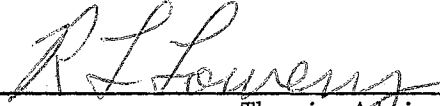
Master of Science  
Oklahoma State University  
Stillwater, Oklahoma  
1963

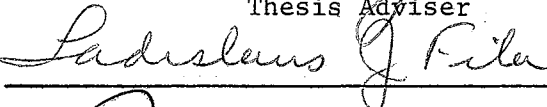
Submitted to the Faculty of the Graduate School of  
the Oklahoma State University  
in partial fulfillment of the requirements  
for the degree of  
DOCTOR OF PHILOSOPHY  
May, 1965

MAY 28 1968

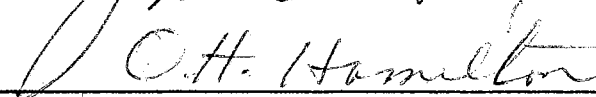
SEPARATION CRITERIA OF A NONLINEAR CONTACT  
SYSTEM IN A STEADY STATE SINUSOIDAL  
VIBRATION ENVIRONMENT

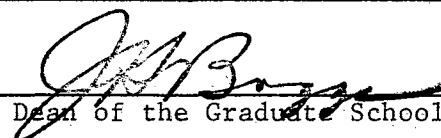
Thesis Approved:

  
\_\_\_\_\_  
Thesis Adviser

  
\_\_\_\_\_

  
\_\_\_\_\_

  
\_\_\_\_\_

\_\_\_\_\_  
  
\_\_\_\_\_  
Dean of the Graduate School

581312

#### ACKNOWLEDGEMENTS

The author wishes to express his thanks and to acknowledge his indebtedness to several people for their roles in the completion of this study.

Particular appreciation is expressed to the thesis adviser, Dr. R. L. Lowery, who gave such patient guidance and encouragement that the author could hardly fail to succeed. Thanks are due Professor L. J. Fila for his many helpful suggestions in the editing of the thesis and to the other committee members, Dr. J. H. Boggs and Dr. O. H. Hamilton.

The author is also indebted to G. W. Cook and G. G. Luton for their aid in the design and construction of the experimental model. Finally, Mrs. Mildred Avery is thanked for the typing of the final manuscript.

## TABLE OF CONTENTS

Chapter	Page
I. INTRODUCTION . . . . .	1
Definition of the Problem . . . . .	1
The Purpose and Scope of the Study . . . . .	2
Previous Work . . . . .	4
II. MATHEMATICAL DERIVATIONS . . . . .	6
The Equation of Motion of the Contact System . . . . .	9
Mathematical Model for Impending Separation . . . . .	10
III. THEORETICAL RESULTS . . . . .	13
Contact Separation Criteria . . . . .	13
Theoretical Frequency Response . . . . .	26
Damping Effects on the Separation Criteria . . . . .	31
IV. EXPERIMENTAL MODEL AND INSTRUMENTATION . . . . .	41
Description of the Model . . . . .	42
Instrumentation . . . . .	45
V. EXPERIMENTAL PROCEDURE AND RESULTS . . . . .	48
Measurement of Model Parameters and Preload . . . . .	48
Measurement of Impending Separation Displacement . . . . .	50
Experimental Results . . . . .	51
Effect of Nonlinear Jump Response on the Separation Criteria . . . . .	60
VI. CONCLUSIONS AND RECOMMENDATIONS . . . . .	68
Recommendations for Further Study . . . . .	69
BIBLIOGRAPHY . . . . .	71
APPENDIX . . . . .	73
A. List of Symbols . . . . .	73
B. List of Major Instrumentation . . . . .	75

LIST OF FIGURES

Figure	Page
1. An Idealized, Preloaded Set of Contacts . . . . .	7
2. Relationship of Separation Displacement to Mass Ratio in the Linear Case. . . . .	15
3. The Influence of Mass Ratio and Nonlinearity of on Separation Displacement. . . . .	17
4. Loci of Points of Vertical Tangency and Corresponding Negative Separation Displacement. . . . .	21
5. The Influence of Preload and Nonlinearity on Separation Displacement . . . . .	23
6. The Influence of Preload and Nonlinearity on Separation Displacement . . . . .	24
7. The Influence of Preload and Nonlinearity on Separation Displacement . . . . .	25
8. Phase Plane Curves for the Free Undamped Response. . . . .	28
9. Damping Force Distribution With Respect to Response Displacement . . . . .	33
10. Effect of Differential Damping Forces on the Separation Criteria . . . . .	34
11. Theoretical Force Between the Contacts as a Function of Displacement. . . . .	36
12. $F_x$ in the Neighborhood of the Point of Vertical Tangency of Fig. 3. . . . .	37
13. $F_x$ in the Neighborhood of the Point of Vertical Tangency of Fig. 7. . . . .	39
14. Schematic of the Test Model . . . . .	42

Figure	Page
15. Block Diagram of Instrumentation . . . . .	46
16. Theoretical and Experimental Displacement for Separation With Varying Frequency . . . . .	52
17. Theoretical and Experimental Displacement for Separation With Varying Frequency . . . . .	53
18. Theoretical and Experimental Displacement for Separation With Varying Frequency . . . . .	54
19. Linear Theoretical and Experimental Displacement for Separation as a Function of Preload . . . . .	56
20. Nonlinear Theoretical and Experimental Displacement for Separation as a Function of Preload . . . . .	57
21. Experimental $\delta_1$ , $\delta_2$ and $\alpha$ . . . . .	58
22. Theoretical Force Between the Contacts . . . . .	59
23. Free Response of the Nonlinear Experimental System. . . . .	61
24. Frequency Domain Response of the Nonlinear Experimental System . . . . .	63
25. Down-Jump Nonlinear Response in the Time Domain . . . . .	65
26. Up-Jump Nonlinear Response in the Time Domain . . . . .	66

LIST OF PLATES

Plate	Page
I. Experimental Model (Side View) . . . . .	43
II. Experimental Model (Top View) . . . . .	44

## CHAPTER I

### INTRODUCTION

The reaction of electrical contacts to vibration fields has taken on added importance with the use of relays and other switching devices in vehicles which inherently produce, or operate in, a vibratory environment. The missile has generated the greatest interest in this area, not only because of the presence of a hostile vibratory environment, but also because of the requirement for a high degree of circuit reliability.

The proper design of switching devices to be used in a vibratory environment requires knowledge of the mechanical reaction of the contacts to the environment. This knowledge, coupled with other design considerations, should enable the designer to avoid or control reactions which would be detrimental. It appears that very little has been done to analyze the vibration effect from a basic mechanical standpoint. Instead, existing configurations have been altered through experimental trial and error for use in a vibratory environment. This approach has met with varying degrees of success. In view of this, a basic study of the mechanical reaction of contacts to a vibratory environment is needed.

#### Definition of the Problem

One problem area associated with contact vibration is that of inadvertent separation of contacts which are held in the closed position by a

set force. The vibratory environment generates forces which overcome the force holding the contacts together. This results in unintentional separation which may introduce a spurious signal into the system.

From a purely mechanical standpoint, the problem is one of controlling the vibration response of the contacts so that they will not separate when subjected to a vibratory excitation. The allowable response for nonseparation may be expected to vary from one contact configuration to another, but limited for all configurations. However, every mechanical system possesses at least one inherent frequency such that, in the absence of damping, excitation at that frequency will theoretically result in unbounded amplitude. Control of the contact amplitude can be accomplished only through energy dissipation with some type of damping.

Since mechanical damping is dependent upon either displacement or velocity, there must be an allowable response amplitude of the contacts without separation if separation is to be prevented in a vibration environment of unlimited frequency range. The problem then becomes one of determining the nonseparation amplitude for a given configuration so that the contact response can be held to a lower amplitude through energy dissipation.

#### The Purpose and Scope of the Study

This study was undertaken to determine the separation criteria for a preloaded, idealized set of contacts when they are subjected to a steady state sinusoidal excitation and when the elasticity of one



contact is nonlinear. The study consists of two phases; theoretical and experimental.

The set of contacts was taken as a two-mass, two-spring system with one nonlinear spring of the Duffing hardening type (1)<sup>1</sup>. With arbitrary system parameters, such a system represents a variety of contact configurations. A linear system is represented by the special case where the nonlinear coefficient becomes zero.

Separation criteria were determined for the contact set under the assumption of negligible damping. The manner in which damping would affect the results was then presented from a qualitative standpoint.

The contact set was idealized by assuming lumped parameters; that is, massless springs and springless masses. The contact preload was assumed without regard to its origin.

The point of impending contact separation is a point of transition from a single degree-of-freedom system to a two degree-of-freedom system. Consequently, it was only necessary to consider the single degree-of-freedom system in determining the separation criteria.

The scope of the theoretical study included the development of the equations of motion of the system; the development of the mathematical model for impending separation of the contacts; a qualitative analysis of system response; the solution of the mathematical model for impending separation in terms of system parameters and preload; and a qualitative analysis of how system damping would affect the results.

---

<sup>1</sup> Numbers in parentheses refer to references of the selected bibliography.

The scope of the experimental study included the design and construction of a large scale model of the contactor system; instrumentation of the model; testing of selected theoretical separation criteria; and investigation of system response within the unstable response regions.

One consequence of the investigation of the unstable system response was the recording of the jump phenomenon in the time domain. A survey of the nonlinear literature indicates that very little is known about the mechanism of jump response. Although it is beyond the scope of this study, an analysis of the jump mechanism made in conjunction with such recordings would be very enlightening and a significant contribution to the nonlinear field.

#### Previous Work

There is no known previous work in the area of contact separation where one contact has a nonlinear elasticity. Separation criteria for linear contacts have been studied and reported (2). However, the approach here is altogether different from that taken in (2) so that a direct comparison of the linear results is not possible.

There have been several notable dynamical studies of specific relays such as (3) and (4) in which contact rebound chatter was considered. However, a vibratory excitation was not considered so the results have little bearing on this study.

Previous work has been accomplished in the area of frequency response for a single degree-of-freedom system with nonsymmetrical restoring force which, as is shown in Chapter III, is the situation for a set of

preloaded contacts with one nonlinear spring. Duffing (5), in his notable work published in 1918, considered such a system, but his work was restricted to the derivation of equations which must be satisfied if the response is to be a biased sinusoid. Rauscher (6) and Den Hartog (7) later devised separate approximate solution techniques based on boundary energy conditions. Ludeke (8) later compared the two solution methods through experimental work and found the method of Rauscher to be the more accurate of the two. Although no general solution resulted from this work, the form of the response was established and is applicable in determining the type of response of the set of contacts under study.

## CHAPTER II

### MATHEMATICAL DERIVATIONS

In this chapter two mathematical models are derived for the preloaded set of contacts when they are subjected to a steady state sinusoidal displacement. They are the equation of motion of the set and the equation of relative displacement for impending separation of the contacts. In both cases, the system is taken as single degree-of-freedom; that is, the contacts do not separate for the defined motion. The limiting case of zero force between the contacts defines the point of impending separation.

By assuming negligible damping, the set of contacts is represented by a two-spring, two-mass system excited by a displacement  $s = s_0 \sin \omega t$  as illustrated in Fig. 1. The parameters  $K$  and  $m_1$  are associated with the nonlinear contact and  $k$  and  $m_2$  with the linear contact. The displacement  $x$  is taken as positive upward and denotes the displacement of the masses from their static equilibrium position with respect to the enclosing case.

For an initial preload of  $F_0$  between the masses, the two springs must exert equal and opposite forces for static equilibrium. The weight of  $m_1$  and  $m_2$  is assumed small in comparison to the preload and is neglected. Therefore, each spring must be in static compression. Let the static compression be  $\delta_1$  in  $K$  and  $\delta_2$  in  $k$ .

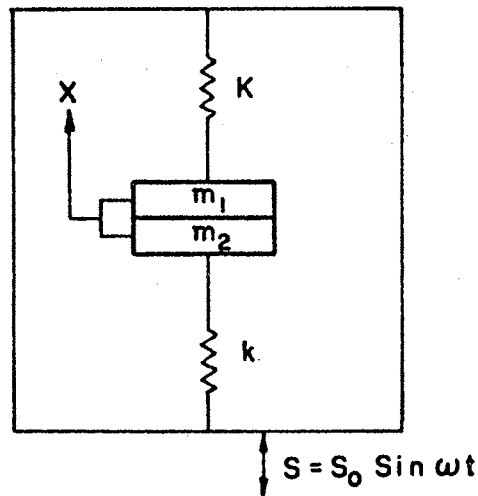


Fig. 1. An Idealized, Preloaded Set of Contacts

Before deriving the desired equations, it is necessary to define the restoring forces of the springs on the masses as a function of the displacement  $x$  and the preload  $F_0$ .

The force exerted by the Duffing-hardening type spring  $K$  on  $m_1$  is

$$F_K = a(y + by^3) \quad ,$$

where  $a$  and  $b$  are both positive and  $y$  is measured positive-upward from the position where  $K$  is unstretched. It follows from the definition of  $\delta_1$  that  $y = x + \delta_1$ . Therefore, the force exerted by  $K$  on  $m_1$  for a displacement  $x$  is

$$F_K = a \{ (x + \delta_1) + b(x + \delta_1)^3 \} \quad . \quad (1)$$

Similarly, the restoring force on  $m_2$  from  $k$  with a displacement  $x$  is

$$F_k = k(x - \delta_2) \quad . \quad (2)$$

The relationship of  $F_o$  to  $\delta_1$  and  $\delta_2$  is given by Equations (1) and (2) when  $x = 0$ . For static equilibrium

$$F_{K/x=0} + F_{k/x=0} = 0 \quad ,$$

which gives

$$F_o = a(\delta_1 + b\delta_1^3) \quad , \quad (3)$$

$$F_o = k\delta_2 \quad . \quad (4)$$

For the sequel it would be advantageous to have Equations (1) and (2) expressed in terms of the preload instead of  $\delta_1$  and  $\delta_2$ . However, this is very difficult in the case of  $\delta_1$  because of the form of Equation (3). There is a one-to-one relationship between  $F_o$  and  $\delta_1$  for all  $\delta_1$  so the inverse function  $\delta_1(F_o)$  does exist. Applying Cardan's formula, the single real value of  $\delta_1$  is given by the following equation: (9)

$$\delta_1 = \left[ \frac{F_o}{2ab} + \left( \frac{1}{27b^3} + \frac{F_o^2}{4a^2b^2} \right)^{1/2} \right]^{1/3} \\ + \left[ \frac{F_o}{2ab} - \left( \frac{1}{27b^3} + \frac{F_o^2}{4a^2b^2} \right)^{1/2} \right]^{1/3} \quad .$$

Substitution of this value for  $\delta_1$  in Equation (1) would unduly complicate the equation. Therefore, Equations (1) and (2) will be left in terms of  $\delta_1$  and  $\delta_2$  with Equations (3) and (4) defining their relationship to the preload.

It is worth noting, however, that for  $b\delta_1^2 \ll 1$ ,  $\delta_1$  is approximately  $\frac{F_o}{a}$ . This is in effect linearizing the static compression in K and would result in little error for small  $F_o$  and/or small  $b$ . This

approximation will not be used here because of the desire to allow  $F_0$  and  $b$  a wide range of values.

### The Equation of Motion of the Contact System

With the restoring forces of the springs defined in terms of  $x$  and the preload, it is now possible to write the equation of motion of the system. Equating forces for the single degree-of-freedom system gives

$$(m_1 + m_2)(\ddot{x} + \ddot{S}) = -F_K - F_k \quad .$$

Expansion of the restoring force terms and rearrangement gives

$$\begin{aligned} \ddot{x} + \frac{a}{m_1+m_2} \left[ \left(1 + \frac{k}{a} + 3b\delta_1^2\right) x + 3b\delta_1 x^2 + bx^3 \right] \\ = -\ddot{S} = S_0 \omega^2 \sin \omega t \quad . \end{aligned} \quad (5)$$

The equation of motion may be written in the more familiar form

$$\ddot{x} + p^2(x + cx^2 + dx^3) = S_0 \omega^2 \sin \omega t \quad , \quad (6)$$

where, in terms of system parameters and preload,

$$p^2 = \frac{a}{m_1+m_2} \left(1 + \frac{k}{a} + 3b\delta_1^2\right) \quad ,$$

$$c = \frac{3b\delta_1}{1 + \frac{k}{a} + 3b\delta_1^2} \quad ,$$

and

$$d = \frac{b}{1 + \frac{k}{a} + 3b\delta_1^2} \quad .$$

The value of  $p$  represents  $2\pi f_n$ , where  $f_n$  is the natural frequency of the system with infinitesimal amplitude.

When  $b$  is set equal to zero (the linear case), Equation (5) reduces to

$$\ddot{x} + \frac{k+a}{m_1+m_2} x = S_0 \omega^2 \sin \omega t \quad (7)$$

which is the equation of motion of a linear, undamped single degree-of-freedom, forced system.

#### Mathematical Model for Impending Separation

For separation of the contacts during vibration, the force between them must change from  $F_0$  at the static equilibrium position ( $x = 0$ ) to zero at the point of impending separation. The varying force between the contacts will be defined as  $F_x$  and each spring-mass considered as a free body. Then, a summation of forces on each mass provides an equation of motion for each spring-mass. The equations are

$$\begin{aligned} m_1(\ddot{x} + \ddot{S}) &= -F_K + F_x, \quad \text{and} \\ m_2(\ddot{x} + \ddot{S}) &= -F_k - F_x. \end{aligned}$$

These equations are valid as long as the system remains single degree-of-freedom or as long as  $|F_x| \geq 0$ . With this restriction, the accelerations may be eliminated between the two equations provided the masses are finite and other than zero. This gives

$$\frac{1}{m_1} (F_K - F_x) = \frac{1}{m_2} (F_k + F_x).$$



Solving for  $F_x$  gives

$$F_x = \frac{m_2 F_K - m_1 F_k}{m_1 + m_2} \quad (8)$$

The use of Equations (1) and (2) and rearrangement gives

$$F_x = \frac{bx^3 + 3b\delta_1 x^2 + (1 + 3b\delta_1^2 - \frac{k}{a} \frac{m_1}{m_2}) x + (\delta_1 + b\delta_1^3 + \delta_2 \frac{k}{a} \frac{m_1}{m_2})}{m_1 + m_2} \quad (9)$$

For the linear case where  $b = 0$ ,  $\delta_1 = \frac{F_o}{a}$  and  $\delta_2 = \frac{F_o}{k}$ , Equation (9) reduces to

$$F_x = \frac{am_2 - km_1}{m_1 + m_2} x + F_o \quad (10)$$

Equation (8) indicates that  $F_x$  can be zero only if the numerator is zero or

$$m_2 F_K - m_1 F_k = 0 \quad (11)$$

The solution of Equation (11) for  $x$  then gives a particular value of  $x$  at which  $F_x$  becomes zero and separation of the contacts is impending. Define this value of  $x$  as  $\bar{X}$ . Substitution from Equations (1) and (2) and rearrangement gives Equation (11) in terms of the impending separation displacement  $\bar{X}$ . It is

$$b\bar{X}^3 + 3b\delta_1 \bar{X}^2 + (1 + 3b\delta_1^2 - \frac{k}{a} \frac{m_1}{m_2}) \bar{X} + (\delta_1 + b\delta_1^3 + \delta_2 \frac{k}{a} \frac{m_1}{m_2}) = 0 \quad (12)$$

For the linear case, Equation (12) reduces to

$$\bar{X} = \frac{F_o (m_1 + m_2)}{m_1 k - m_2 a} \quad (13)$$

In summary, the response of the set of contacts is given by the solution of Equation (6) for the condition where separation does not occur; that is, the equation is only valid for a response amplitude  $\leq \bar{X}$ . The value of  $\bar{X}$  is represented by the zeros of Equation (9). Where Equation (9) has more than one real zero, it is the real zero with the smallest absolute value that determines the point of impending separation.

It is noteworthy that all of the equations pertaining to the force between the contacts are independent of the contact masses. Each equation may be expressed in terms of the dimensionless mass ratio.

## CHAPTER III

### THEORETICAL RESULTS

In this chapter the theoretical separation criteria for the undamped set of contacts are determined, the effect of contact damping on the criteria is investigated, and the general type of frequency response of the set of contacts to the steady state sinusoidal excitation is presented.

#### Contact Separation Criteria

The contact separation criteria are obtained from the solution of Equation (12) for the displacement  $\bar{X}$  in terms of the system parameters and preload. It is evident that the complexity of Equation (12) prevents a general solution. Therefore, it is necessary to select a given parameter as an independent variable and hold the others constant while solving for the dependent variable  $\bar{X}$ .

Before attacking Equation (12), it is convenient to determine the separation criteria for the linear case represented by Equation (13). Since the equation was developed under the restriction that neither mass could be zero or infinite, it may be rewritten in the form

$$\bar{X} = \frac{F_0}{a} \frac{\frac{m_1}{m_2} + 1}{\frac{m_1}{m_2} \frac{k}{a} - 1}$$

For the condition  $\frac{k}{m_2} = \frac{a}{m_1}$ ,  $\bar{X}$  is unbounded and there is no displacement for impending separation of the contacts. For this condition the natural frequencies of the two contacts must be equal because  $\frac{a}{m_1}$  and  $\frac{k}{m_2}$  are the squares of the respective natural circular frequencies. Consequently, the mathematical model implies that the contacts will not separate if they have the same natural frequency. As the stiffness of either spring tends to infinity,  $\bar{X}$  tends to zero. Infinite stiffness corresponds to the condition of a rigid contact. Therefore, the configuration of a flexible contact against a rigid contact permits no motion without separation and there can be no energy dissipation through mechanical damping without separation.

Since all parameters are independent of  $F_0$ ,  $\bar{X}$  is directly proportional to the preload. The effect of varying mass is not so apparent. If the effect of varying mass ratio,  $\frac{m_1}{m_2}$ , is considered, the equation plots as rectangular hyperbolas which are asymptotic to the lines  $\bar{X} = \frac{F_0}{k}$  and  $\frac{m_1}{m_2} = \frac{a}{k}$  as shown in Fig. 2. As the mass ratio becomes very small,  $\bar{X}$  approaches  $-\frac{F_0}{a}$  which is the unstretched position of the upper spring. As the ratio becomes large,  $\bar{X}$  approaches  $\frac{F_0}{k}$  which is the unstretched position of the lower spring. These conditions imply that the top spring must be in tension for separation in the negative direction and that the bottom spring must be in tension for separation in the positive direction. In general, the absolute displacement for separation for  $\frac{m_1}{m_2}$  is not equal to that for  $\frac{m_2}{m_1}$ . However, if  $\frac{a}{k}$  is unity, the absolute separation displacements are the same.

Returning to the nonlinear case represented by Equation (12), it is seen that here too the system parameters and preload are independent

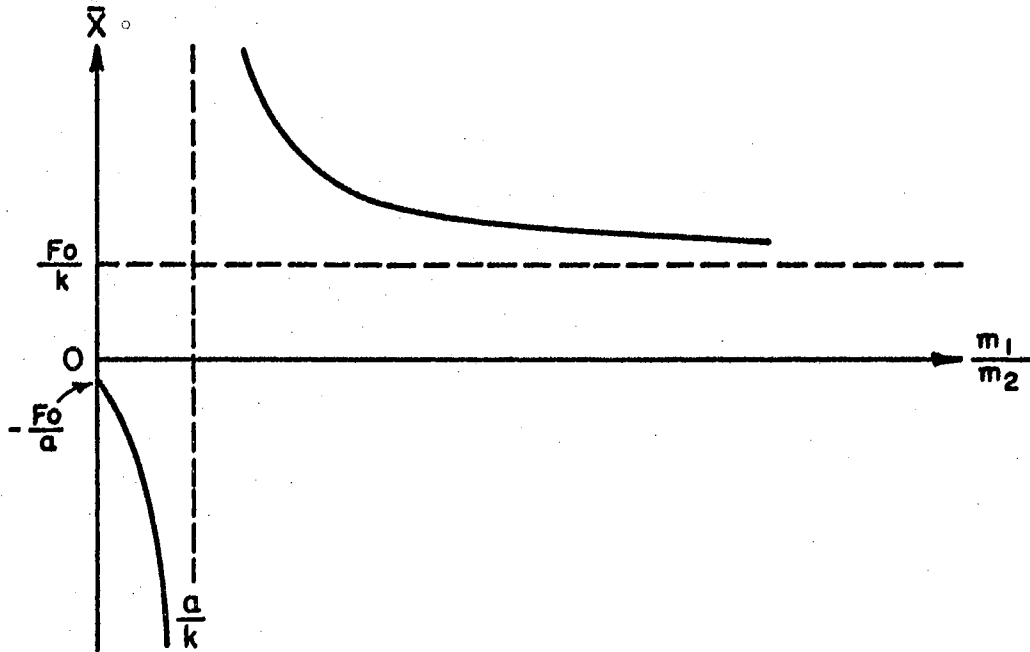


Fig. 2. Relationship of Separation Displacement to Mass Ratio in the Linear Case

of the mass ratio,  $\frac{m_1}{m_2}$ . Furthermore, the equation is also linear in  $\frac{m_1}{m_2}$  so that it is possible to express  $\frac{m_1}{m_2}$  as an explicit function of  $\bar{X}$ , whereas, it is not possible to express  $\bar{X}$  as an explicit function of  $\frac{m_1}{m_2}$ . The solution of Equation (12) for  $\frac{m_1}{m_2}$  gives

$$\frac{m_1}{m_2} = \frac{a \{ b\bar{X}^3 + 3b\delta_1\bar{X}^2 + (1 + 3b\delta_1^2)\bar{X} + (\delta_1 + b\delta_1^3) \}}{k(\bar{X} - \delta_2)} \quad (14)$$

The fact that  $\bar{X}$  has become the independent variable presents no problem in showing the dependence of  $\bar{X}$  on  $\frac{m_1}{m_2}$ . The role of the two is merely reversed in plotting their relationship.

Little can be done in plotting Equation (14) without resorting to numerical values for the remaining parameters and preload. Even this

is not entirely satisfactory because  $\delta_1$  is related to  $F_0$  through the cubic of Equation (3). However, by assigning numerical values to  $F_0$ ,  $a$ ,  $b$ , and  $k$  it is possible to obtain the relationship of  $\bar{X}$  to the mass ratio by use of the digital computer. The values so obtained are plotted in Fig. 3 for five values of  $b$  where the solid lines represent the smallest absolute value of  $\bar{X}$  and dashed lines represent the values which could not be physically attained before separation.

Figure 3 shows that  $\bar{X}$  is bounded for  $b \neq 0$  and that the greatest absolute bound becomes progressively smaller as the nonlinearity increases. It also shows that the points of vertical tangency to the upper curves represent an important demarcation in the allowable displacement for nonseparation. As an example, at point 1 on the  $b = 100$  curve, separation will occur when the displacement is about -0.45 inches. However, for a slightly larger value of  $\frac{m_1}{m_2}$ , point 2, the point of vertical tangency to the  $b = 100$  curve, shows separation at about 0.09 inches displacement. This represents an abrupt decrease in the allowable nonseparation displacement and illustrates the importance of the point of vertical tangency to the upper curve.

The points of vertical tangency to the upper curve are given by the condition where  $\frac{d\bar{X}}{d(\frac{m_1}{m_2})} \rightarrow \infty$ . If Equation (12) is set equal to  $f(\frac{m_1}{m_2}, \bar{X})$ ,  $\frac{d\bar{X}}{d(\frac{m_1}{m_2})}$  is given by

$$\frac{d\bar{X}}{d(\frac{m_1}{m_2})} = - \frac{\partial f / \partial (\frac{m_1}{m_2})}{\partial f / \partial \bar{X}} = \frac{k}{a} \frac{\bar{X} - \delta_1}{3b\bar{X}^2 + 6b\delta_1\bar{X} + (1 + 3b\delta_1^2 - \frac{k}{a}\frac{m_1}{m_2})} \quad (15)$$

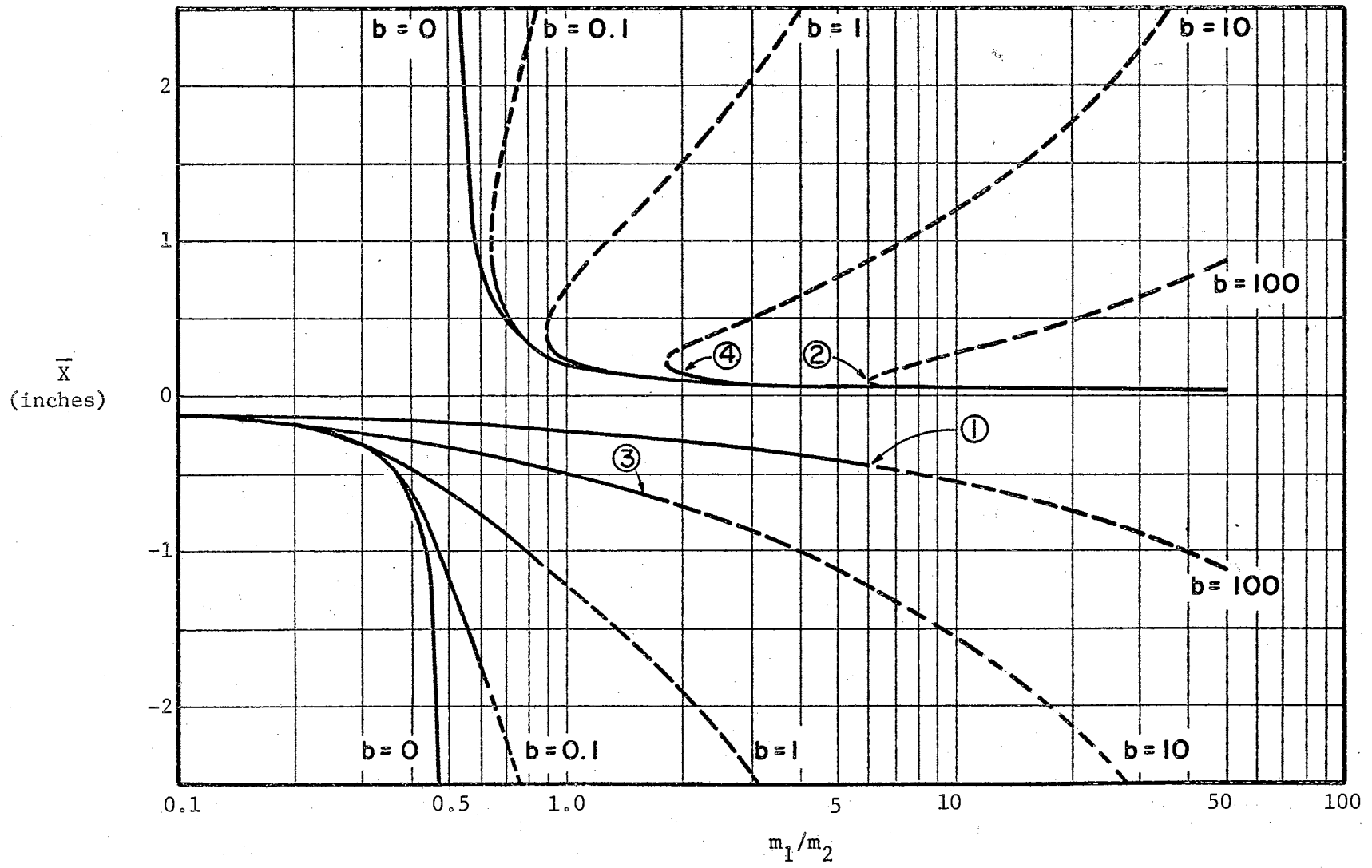


Fig. 3. The Influence of Mass Ratio and Nonlinearity on Separation Displacement,  $a = 100$  lb/in,  
 $k = 200$  lb/in,  $F_0 = 10$  lbs

The value of the derivative will approach infinity only when the denominator approaches zero. If the denominator is set equal to zero, the value of  $\bar{X}$  is

$$\bar{X} = -\delta_1 \pm \sqrt{\frac{1}{3b} \left( \frac{k}{a} \frac{m_1}{m_2} - 1 \right)} \quad (16)$$

Equation (16) is double valued, but the positive sign in front of the radical must hold in determining the desired points of vertical tangency to the upper branch of each curve of Fig. 3 because each point of vertical tangency has a positive  $\bar{X}$  coordinate. If the negative sign held,  $\bar{X}$  would be negative. The curves of Fig. 3 are based on numerical examples and do not represent the general case. However, it is easily shown by Descartes' Rule of Signs that the double valued branch of Equation (12) must be associated with a positive value of  $\bar{X}$  in general. Since all of the parameters of Equation (12) are positive, the coefficients must be positive with the possible exception of the coefficient of the  $\bar{X}$  term. Therefore, there will be either zero or two sign changes for all positive values of  $\frac{m_1}{m_2}$ . The Rule then states that there will be either two or no real positive zeros of Equation (12). This then implies that the point of vertical tangency is associated with a positive value of  $\bar{X}$  and that the negative sign in front of the radical has no meaning in determining the points of vertical tangency.

The points of vertical tangency are determined by a simultaneous solution of Equations (12) and (16). The complexity of the two equations is such that a general solution cannot be obtained. However, the points may be obtained for numerical examples such as those from which the curves of Fig. 3 were obtained. An iterative digital computer



solution based on arbitrary values of  $\frac{m_1}{m_2}$  appears to be the simplest method for finding the points. Such a solution method requires a starting point for  $\frac{m_1}{m_2}$  so that convergence will be rapid and certain. A logical starting value of  $\frac{m_1}{m_2}$  is that value where Equation (16) gives a zero value of  $\bar{X}$ . The starting value is then

$$\frac{m_1}{m_2} = \frac{a}{k} (1 + 3b\delta_1^2)$$

If Equation (12) is set equal to  $F$ , the point of vertical tangency is defined when  $F$  is equal to zero for values of  $\frac{m_1}{m_2}$  and  $\bar{X}$  which satisfy Equation (16). If the starting value of  $\frac{m_1}{m_2}$  and  $\bar{X} = 0$  are substituted into Equation (12),  $F$  is positive. As larger values of  $\frac{m_1}{m_2}$  are substituted into Equation (16),  $\bar{X}$  will increase. As the larger values of  $\frac{m_1}{m_2}$  and  $\bar{X}$  which satisfy Equation (16) are substituted into Equation (12),  $F$  will approach zero. However, if the values of  $\frac{m_1}{m_2}$  and  $\bar{X}$  which satisfy Equation (16) are larger than those which define the point of vertical tangency,  $F$  will be negative. This is the basis for the computer solution.

In the computer solution, Equation (16) is solved for  $\bar{X}$  for the starting value of  $\frac{m_1}{m_2}$ . These values of  $\bar{X}$  and  $\frac{m_1}{m_2}$  are substituted into Equation (12) which is solved for  $F$ . The absolute value of  $F$  is then compared to an allowable tolerance from zero, say  $10^{-6}$ . If  $|F|$  is greater than  $10^{-6}$ ,  $\frac{m_1}{m_2}$  is increased by a small increment and the process is repeated until  $|F|$  becomes equal to or less than  $10^{-6}$ , or  $F$  becomes negative and  $|F| > 10^{-6}$ . If the latter occurs, further increases in  $\frac{m_1}{m_2}$  would cause divergence of  $|F|$ ; therefore,  $\frac{m_1}{m_2}$  is

decreased by the last increment and then increased by smaller increments. Through repetition,  $|F|$  converges to  $10^{-6}$  and the point of vertical tangency is approximately defined.

The above solution gives only the point of vertical tangency to the upper branch of the solution of Equation (12). The effect of  $\bar{X}$  becoming triple valued at this point is not presented unless the corresponding negative value of  $\bar{X}$  is known. Therefore, it is necessary to substitute the  $\frac{m_1}{m_2}$  value of the point of vertical tangency into Equation (12) and solve the resulting cubic in  $\bar{X}$  for the negative value of  $\bar{X}$ .

The loci of the vertical tangents for three values of preload are plotted in Fig. 4 along with the loci of values of negative  $\bar{X}$  corresponding to the points. The curves give a general idea of how the points of vertical tangency shift with preload and nonlinearity.

Probably the most important parameter affecting the separation displacement is the preload. It was shown in the linear case that the separation displacement was linearly dependent on preload. The effect in the nonlinear case is less evident because the preload is buried in  $\delta_1$  and  $\delta_2$  of Equation (12). However, it is possible to determine the relation of separation displacement to preload with numerical examples by allowing  $\delta_1$  to be the independent variable. With fixed  $a$ ,  $b$ ,  $k$  and  $\frac{m_1}{m_2}$ , Equation (12) is solved for  $\bar{X}$ , Equation (3) for  $F_0$ , and Equation (4) for  $\delta_2$  for each value of  $\delta_1$ . Then a plot of  $\bar{X}$  versus  $F_0$  presents the desired relationship.

The solution of Equation (12) for  $\bar{X}$  in terms of  $\delta_1$  is not as simple as it was for  $\bar{X}$  in terms of  $\frac{m_1}{m_2}$  because the equation is not

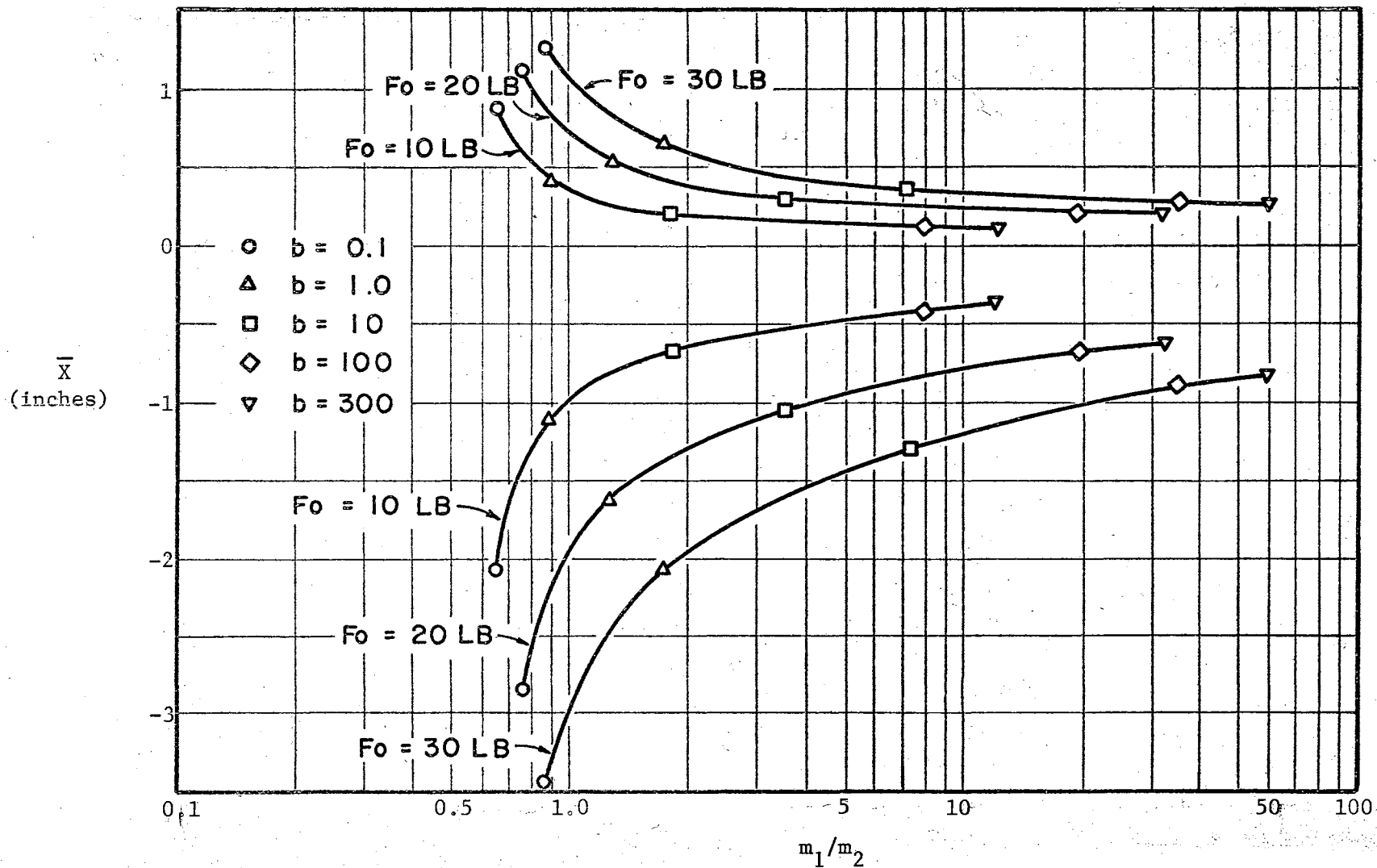


Fig. 4. Loci of Points of Vertical Tangency and Corresponding Negative Separation Displacement,  $a = 100$  lb/in,  $k = 200$  lb/in.

linear in  $\delta_1$ . It must be solved by computing the coefficients of the equation for each value of  $\delta_1$  and then solving the resulting cubic for  $\bar{X}$ . Figures 5, 6, and 7 show such solutions where  $a$ ,  $b$  and  $k$  have the values used in the solution of Equation (14) and  $\frac{m_1}{m_2}$  has values of particular interest. The value of  $\frac{m_1}{m_2}$  used in Fig. 5 is the value where  $\bar{X}$  is theoretically unbounded and independent of  $F_0$  for the linear case. The curves illustrate that preload has less effect on  $\bar{X}$  as the nonlinearity increases. The values of  $\frac{m_1}{m_2}$  used in Figs. 6 and 7 illustrate the theoretical triple values of  $\bar{X}$  associated with the nonlinearity.

If Equation (12) is thought of as a relationship of  $\bar{X}$ ,  $F_0$  and  $\frac{m_1}{m_2}$ , the equation defines a set of surfaces for each value of the remaining parameters. Then, if Fig. 3 is considered to have the third dimension  $F_0$  going into the paper, the curves for each value of  $b$  represent a cut across the  $(\bar{X}, F_0, \frac{m_1}{m_2})$  surface at  $F_0 = 10$  lb. Similarly, Figs. 5, 6 and 7 represent surface cuts by the planes  $\frac{m_1}{m_2} = 0.5, 1.0$  and  $5.0$  respectively. Consequently, the four figures provide a representation of the  $(\bar{X}, F_0, \frac{m_1}{m_2})$  surface defined by Equation (12). This representation plus the effect depicted by Fig. 4, present the separation criteria in terms of preload and all system parameters except  $a$  and  $k$ .

The ratio of  $a$  and  $k$  has little meaning as a separate parameter because  $\delta_1$  is dependent upon  $a$ . The effect of varying  $k$  by itself can be determined easily from Equation (14) where the numerator is independent of  $k$ . The denominator,

$$k(x - \delta_2) = kx - F_0 \quad ,$$

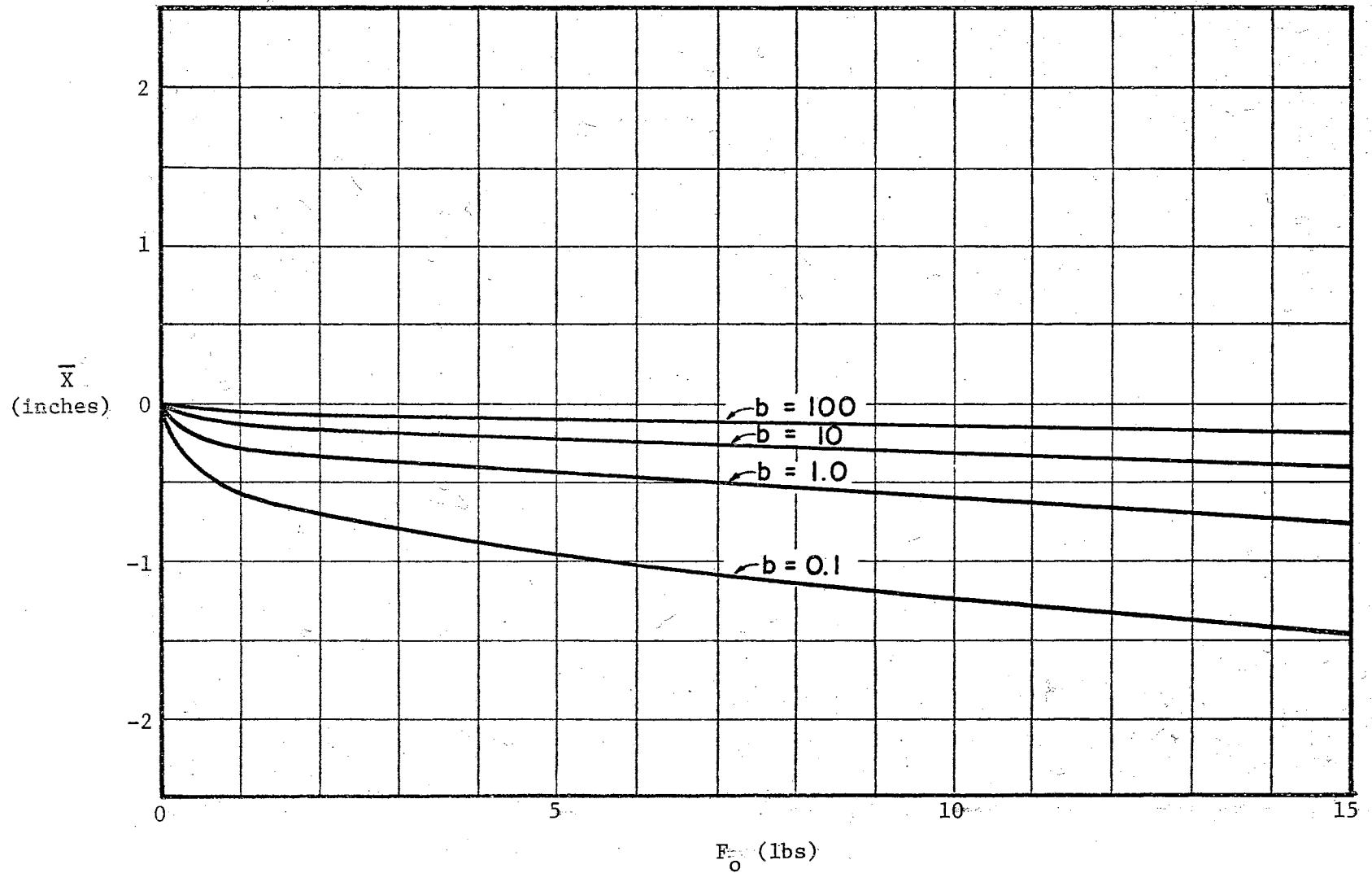


Fig. 5. The Influence of Preload and Nonlinearity on Separation Displacement,  
 $a = 100 \text{ lb/in}$ ,  $k = 200 \text{ lb/in}$ ,  $m_1/m_2 = 0.5$

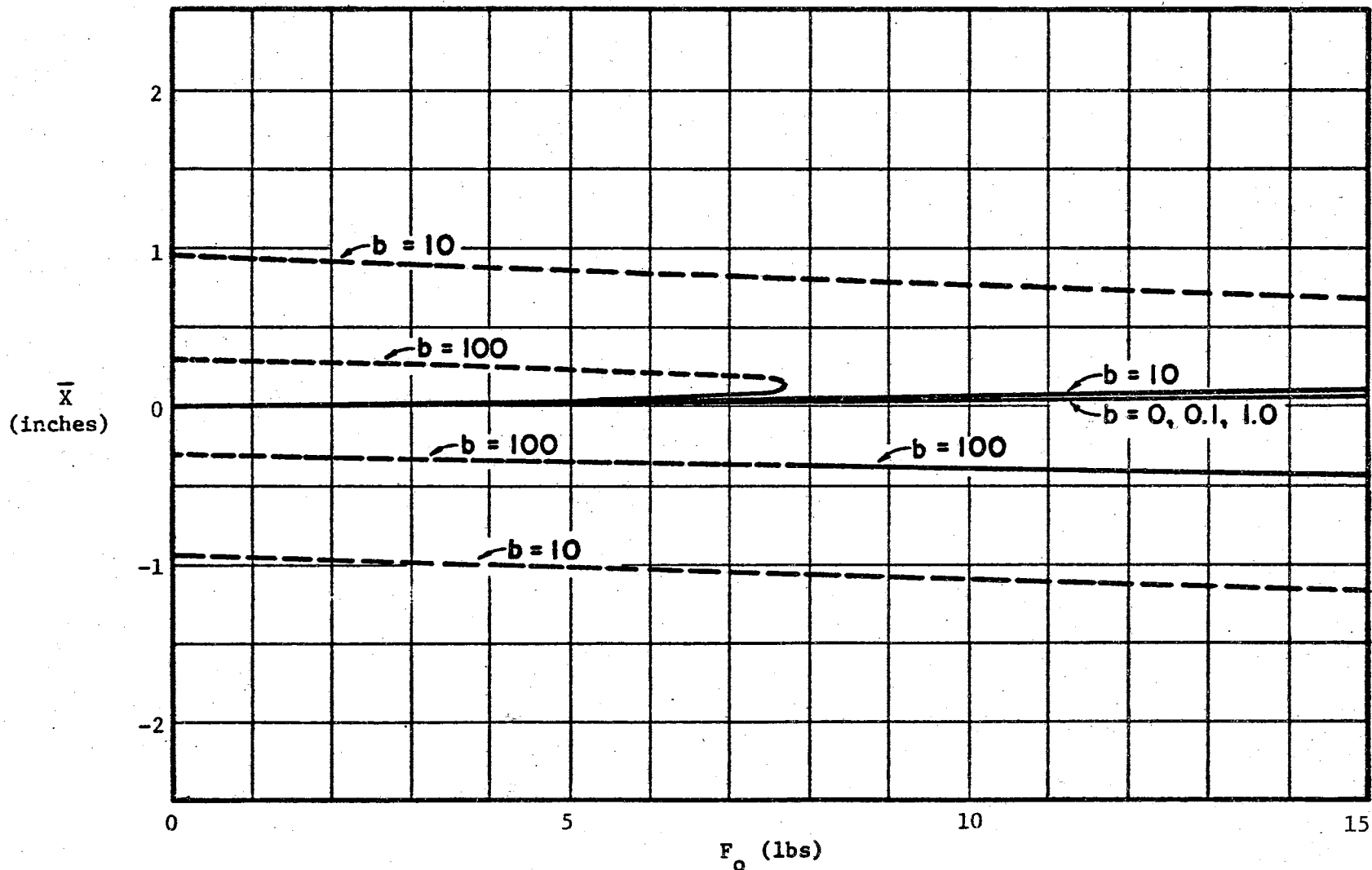


Fig. 6. The Influence of Preload and Nonlinearity on Separation Displacement,  
 $a = 100$  lb/in,  $k = 200$  lb/in,  $m_1/m_2 = 5$

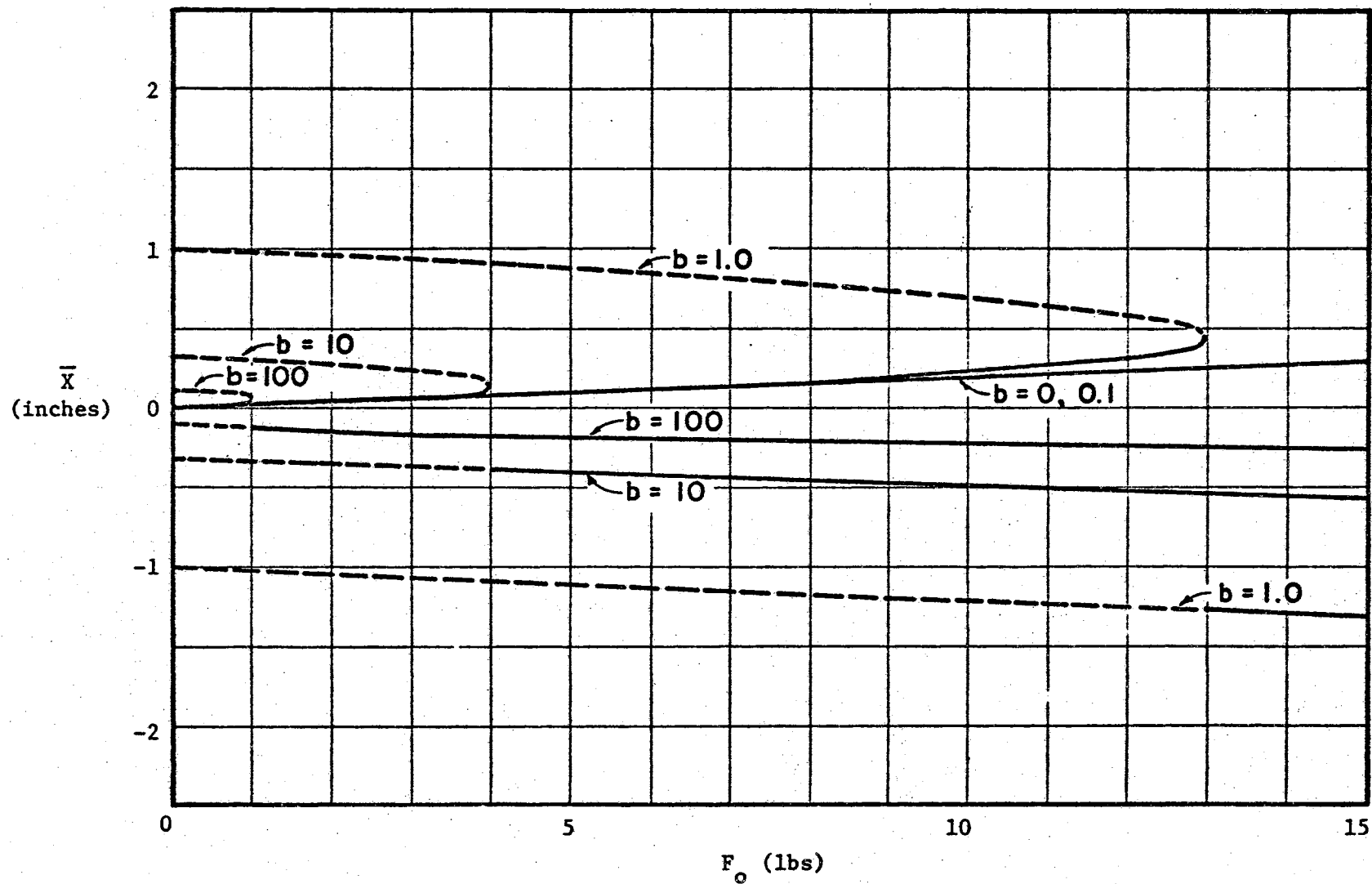


Fig. 7. The Influence of Preload and Nonlinearity on Separation Displacement,  
 $a = 100$  lb/in,  $k = 200$  lb/in,  $m_1/m_2 = 1$

has the effect of expanding or contracting the  $\frac{m_1}{m_2}$  axis for varying  $k$ . The effect from varying  $a$  is less apparent. An exact determination of the effect could be determined by much the same procedure as that used in determining the effect of  $F_0$ . By allowing  $\delta_1$  to be independent, a value of  $a$  would be obtained from Equation (3) for fixed  $F_0$  and  $b$ . This value of  $a$  and  $\delta_1$  along with the fixed parameters would determine the coefficients of Equation (12) which could then be solved for  $\bar{X}$ . The plot of  $\bar{X}$  versus  $a$  would then determine the effect of varying  $a$  on the separation displacement for one set of conditions. However, a sufficient understanding of the effect can be obtained from inspection of the linear case as shown in Fig. 2.

#### Theoretical Frequency Response

Before investigating the effect of damping on the separation criteria determined for the undamped system, it is necessary to find the nature of time response which the set of contacts will have to the steady state sinusoidal excitation.

Inspection of the equation of motion of the set of contacts, Equation (5), reveals the nonsymmetry of the elastic restoring forces about the static equilibrium position of the preloaded contacts. The nonsymmetry stems from the  $x^2$  term which exerts a restoring force which is independent of the direction of displacement from the static equilibrium position. With the orientation shown in Fig. 1 this force is always directed downward. This implies that for a given positive displacement from the static equilibrium position the restoring force on the masses will be greater in magnitude than for the same negative displacement.



One important consequence of the nonsymmetry of the restoring forces is that a combination of hardening and softening is present in the preloaded set of contacts. Hardening is defined as an increase of stiffness with displacement and softening a decrease. Stiffness is the change of force magnitude with respect to displacement. The restoring forces are symmetrical and hardening when measured from the unstretched position of the nonlinear spring at  $x = -\delta_1$ . Therefore, the restoring forces measured from  $x = 0$  must be softening for  $-x < \delta_1 < 0$  and hardening for all other  $x$ . As a result, the response must have a combination of softening and hardening characteristics.

Some knowledge of the response can be gained from a phase plane plot of the undamped free oscillations of the contacts. After assigning numerical values to the system parameters and preload and setting the forcing function equal to zero, the approximate phase plane curves can be obtained from Equation (5) by a digital computer solution based on the phase plane delta method (10). The resulting curves are the loci of constant energy and are approximately ellipses similar to those shown in Fig. 8.

The type of time response represented by the phase plane curves can be determined from the fact that simple harmonic motion is represented in the phase plane as an exact ellipse (1). Assuming the curves to be exact ellipses, the response is simple harmonic motion about the minor axis of each ellipse. The time response is then given by

$$x = \alpha + \beta \sin \Omega t \quad (17)$$

where  $\alpha$  is the  $x$  coordinate of the minor axis of the elliptic curve.

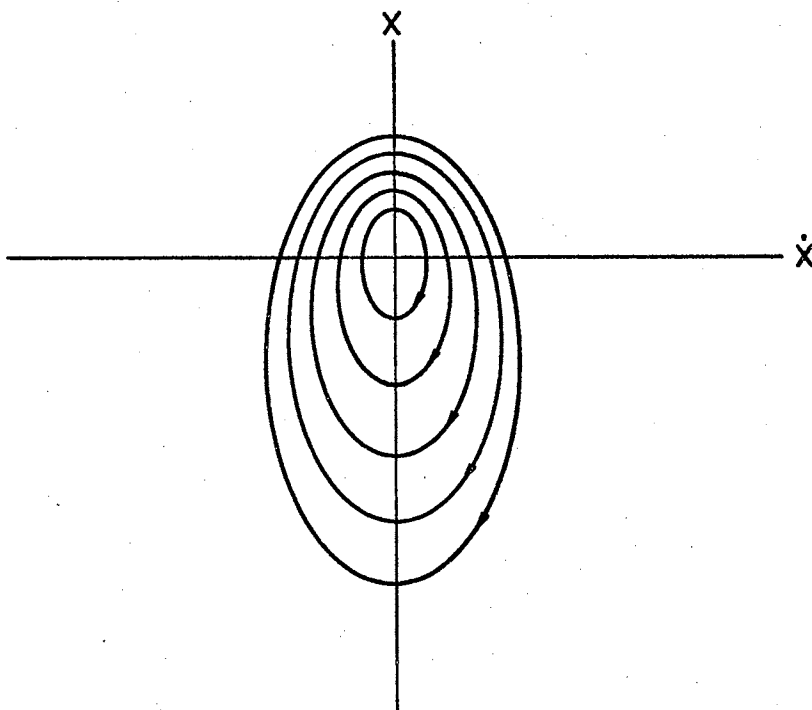


Fig. 8. Phase Plane Curves for the Free Undamped Response

The relationship between  $\alpha$  and  $\beta$  may be found through energy considerations. At the points  $(0, \alpha + \beta)$  and  $(0, \alpha - \beta)$  the energy is entirely potential and equal. For the free system the following equality must hold,

$$\int_0^{\alpha+\beta} (F_K + F_k) dx = \int_0^{-(\alpha-\beta)} (F_K + F_k) dx \quad ;$$

where the integrands are the sum of Equations (1) and (2). The relationship between  $\alpha$  and  $\beta$  is then:

$$b\alpha^3 + 3b\delta_1\alpha^2 + \left(1 + \frac{k}{a} + 3b\delta_1^2 + b\beta^2\right)\alpha + b\delta_1\beta^2 = 0 \quad .$$

Since the equation is linear in  $\beta^2$ , it may be written as

$$\beta^2 = - \frac{b\alpha^3 + 3b\delta_1\alpha^2 + (1 + \frac{k}{a} + 3b\delta_1^2)\alpha}{b(\alpha + \delta_1)} \quad (18)$$

In this form it may be seen that  $\beta^2$  is negative for all positive  $\alpha$  so that  $\beta$  is imaginary. This implies that  $\alpha$  must always be negative which agrees with the results shown in Fig. 8. Letting  $\gamma = -\alpha$ , the equation becomes

$$\beta^2 = \frac{b\gamma^3 - 3b\delta_1\gamma^2 + (1 + \frac{k}{a} + 3b\delta_1^2)\gamma}{b(\delta_1 - \gamma)}$$

The limits of  $\beta^2$  are zero for  $\gamma = 0$  and infinite for  $\gamma = \delta_1$ .  $\beta^2$  is monotonic increasing for  $0 < \gamma < \delta_1$  as may be verified from the positive sign of  $d\beta^2/d\gamma$ . From this it may be concluded that the biasing will increase with free vibration amplitude and that its value will lie between zero and  $-\delta_1$ . Referring back to Fig. 1, it is implied from the latter conclusion that the nonlinear spring  $K$  will be in compression for the point about which the oscillation is taking place.

The foregoing was based on the assumption that the phase plane curves were perfect ellipses. The fact that they are not indicates that higher harmonics must be added to Equation (17) to account for the distortion of the curves. Since it is the velocity distribution with respect to displacement which will be used in the qualitative investigation of damping effects on the separation criteria, it will be sufficiently accurate to neglect the slight harmonic distortion. Therefore, it will be assumed that Equation (17) defines the contact response.

In the case of the forced vibration of the system, the form of the response is essentially the same as that of the free vibration. However, the relationship between  $\alpha$  and  $\beta$  is slightly different. Duffing (5) shows that in the case of forced vibration of a nonsymmetrical system  $\beta^2$  is two-thirds of that shown in Equation (18). This indicates that for a given response amplitude the biasing will be about 22 per cent greater. The difference in biasing between the free and forced cases stems from the condition that, although there can be no net energy transfer during a cycle without damping, there can be energy added during a part of a cycle and removed during the remainder of the cycle.

The conclusions reached regarding the biasing in the free case are also valid for the forced case because Equation (18) has been changed only by a constant multiplying factor.

The type of time response to be expected for the nonlinear contacts has been established with one possible exception. It is well known that there is a jump phenomenon associated with the response of a nonlinear system. Stoker (1) and many others have explored the jump phenomenon in much detail for the frequency domain but it appears that little is known about it in the time domain. This raises the question of the possibility of the separation criteria being altered by inertia forces associated with the jumps. This possibility is explored during the experimental phase.

From the foregoing it can be predicted that, with the possible exception of the jump region, the response of the nonlinear contacts will be essentially a biased sinusoid as given by Equation (17).

### Damping Effects on the Separation Criteria

It is necessary to determine the effect of damping on the separation criteria which have been established for the undamped contacts. If separation is to be prevented over an unlimited frequency range of excitation, it is necessary that the response of the contacts be less than that which will cause separation. However, the contact response can be limited only if there is damping to dissipate energy. If the application of damping were to decrease the allowable nonseparation displacement, the benefits from limiting the response would be nullified.

The effects from viscous, structural and friction damping will be considered. Viscous damping is proportional to velocity; structural damping is taken as proportional to displacement; and friction damping is constant (11). The force generated by each type is 180 degrees out of phase with the velocity.

It is clear that equal damping forces on the two contacts will not affect the force between the contacts because they both have the same velocity for nonseparation. Therefore, it is only the difference between damping forces that will alter the separation criteria established for the undamped case.

With damping present, the point of impending separation becomes that point at which the sum of the undamped force between the contacts,  $F_x$ , and the difference between the damping forces,  $F_d$ , becomes zero. Since  $F_x$ , as given by Equations (9) and (10), is with respect to the displacement  $x$ , it is convenient to look at the difference of damping forces,  $F_d$ , as a function of displacement.

Figure 9 (a) shows the damping force distribution for unequal structural damping for a negative velocity. For positive velocity, the distribution is the image of the lines in the x axis. Figure 9 (b) is the difference of the two force distributions. The subscripts 1 and 2 refer to the upper and lower contacts respectively. Figures 9 (c) and (d) show the distribution for the difference of damping forces for viscous and friction damping respectively. In each case the response is assumed to be that of Equation (17).

All of the damping force distributions of Fig. 9 are double valued with respect to displacement because the velocity changes signs at  $\alpha - \beta$  and  $\beta - \alpha$ . Therefore, if  $F_d$  is adding to  $F_x$  for positive velocity, it is subtracting for negative velocity and vice versa. Consequently,  $F_d$  must be considered as always subtracting from the  $F_x$  distribution in determining the point where the force between the contacts becomes zero with differential damping forces present. Now define this point as  $\bar{X}'$  so that it can be compared with the undamped separation displacement  $\bar{X}$ . In order to determine  $\bar{X}'$  it is necessary to compare the  $F_x$  and  $F_d$  distributions. It is convenient to assume subsequent plots of  $F_x$  and  $F_d$  to be of opposite signs so that the intersection of the two curves defines  $\bar{X}'$ .

In the linear case, the  $F_x$  distribution is given by the linear Equation (10). For  $m_1 k > m_2 a$ ,  $\bar{X}$  is positive as shown in Fig. 10. Figure 10 (a) shows how the differential damping force distribution associated with unequal structural damping has decreased the allowable response for nonseparation. Figures 10 (b) and (c) show the effects for differential viscous and friction damping forces.

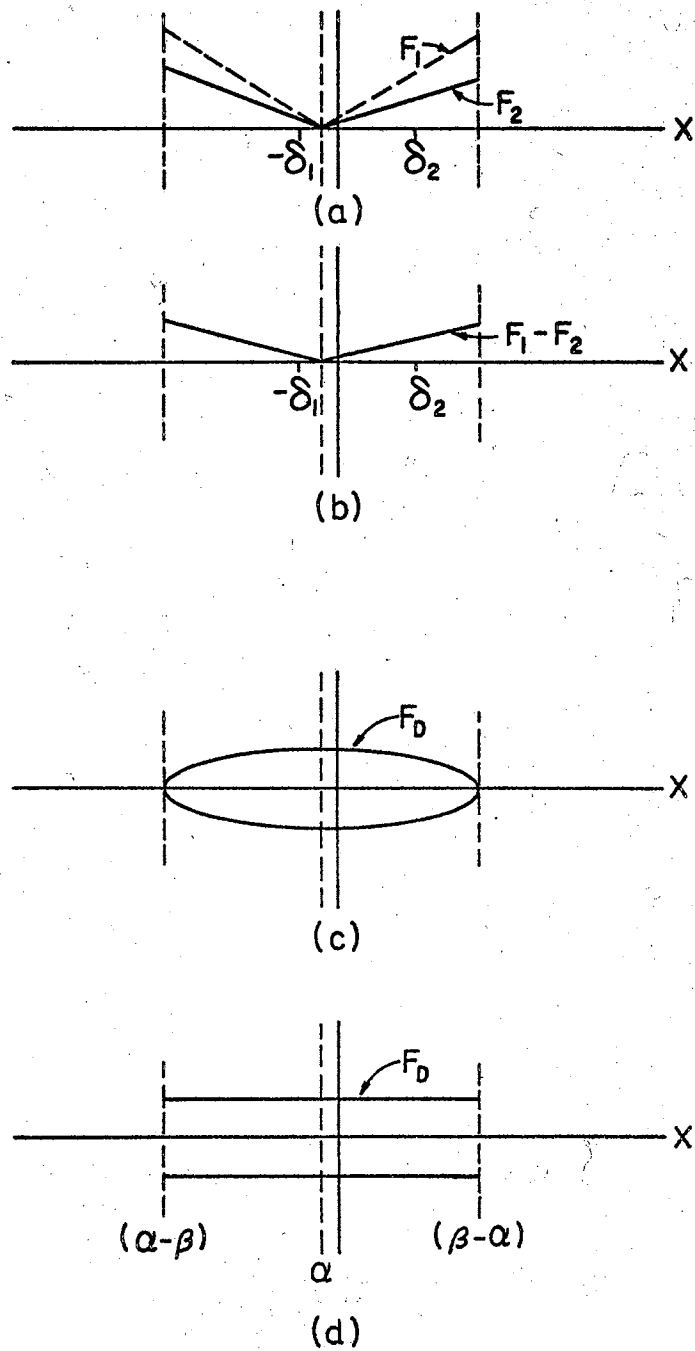


Fig. 9. Damping Force Distribution With Respect to Response Displacement

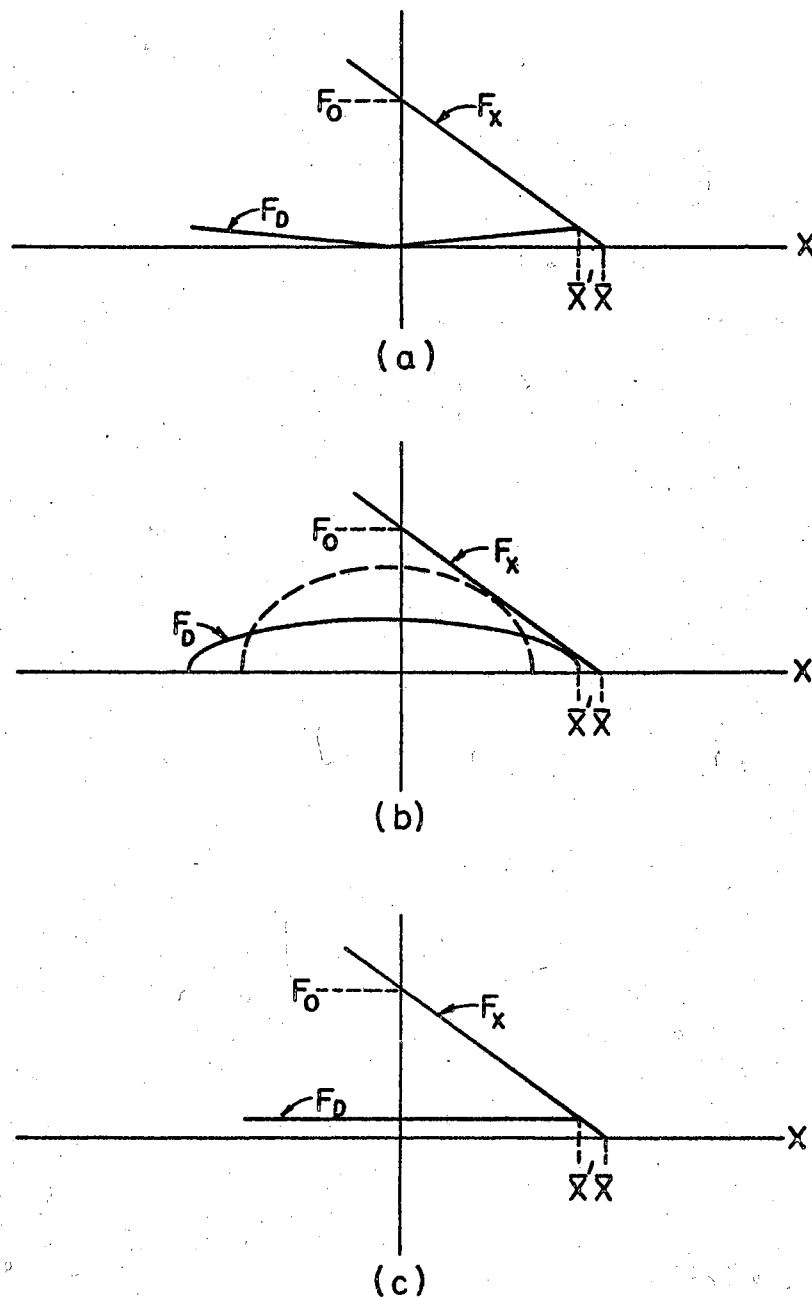


Fig. 10. Effect of Differential Damping Forces on the Separation Criteria.



Figure 10 (b) illustrates the single case where the exciting frequency may influence  $\bar{X}'$  because the velocity is a function of frequency. With a constant difference between the viscous damping coefficients, the eccentricity of the elliptic  $F_d$  distribution decreases as the response frequency increases. This decreases  $\bar{X}'$  as shown by the exaggerated dashed  $F_d$  curve of Fig. 10 (b).

In the nonlinear case, the  $F_x$  distribution is given by Equation (9). The complexity of the equation prevents the simple representation used in the linear case. However, numerical examples may be plotted so that an idea may be obtained of how the difference in damping will affect the separation criteria. Such a numerical case is shown in Fig. 11 for the parameters and preload shown. If the  $F_d$  distribution were as shown, separation would occur at  $\bar{X}'$  instead of at  $\bar{X}$ .

Figure 3 shows on the  $b = 10$  curve that  $\bar{X}$  has the value of point 3, the point of vertical tangency and point 4 respectively for  $\frac{m_1}{m_2} = 1.5, 1.805$  and  $2$ . Figure 12 shows the values of  $F_x$  for positive  $x$  in the neighborhood of the point of the vertical tangency for these values of  $\frac{m_1}{m_2}$ . If the  $F_d$  distribution were as shown in Fig. 12,  $\bar{X}'$  would be as shown for the  $\frac{m_1}{m_2} = 2.0$  curve. The intersection of the  $F_d$  line with the  $\frac{m_1}{m_2} = 1.805$  line would determine  $\bar{X}'$  for that configuration. The  $F_d$  distribution would not cause separation of the  $\frac{m_1}{m_2} = 1.5$  configuration for a positive displacement. However, it would cause separation at a smaller absolute value of negative displacement than that predicted for the undamped case. Any value of  $F_d$  would have the effect

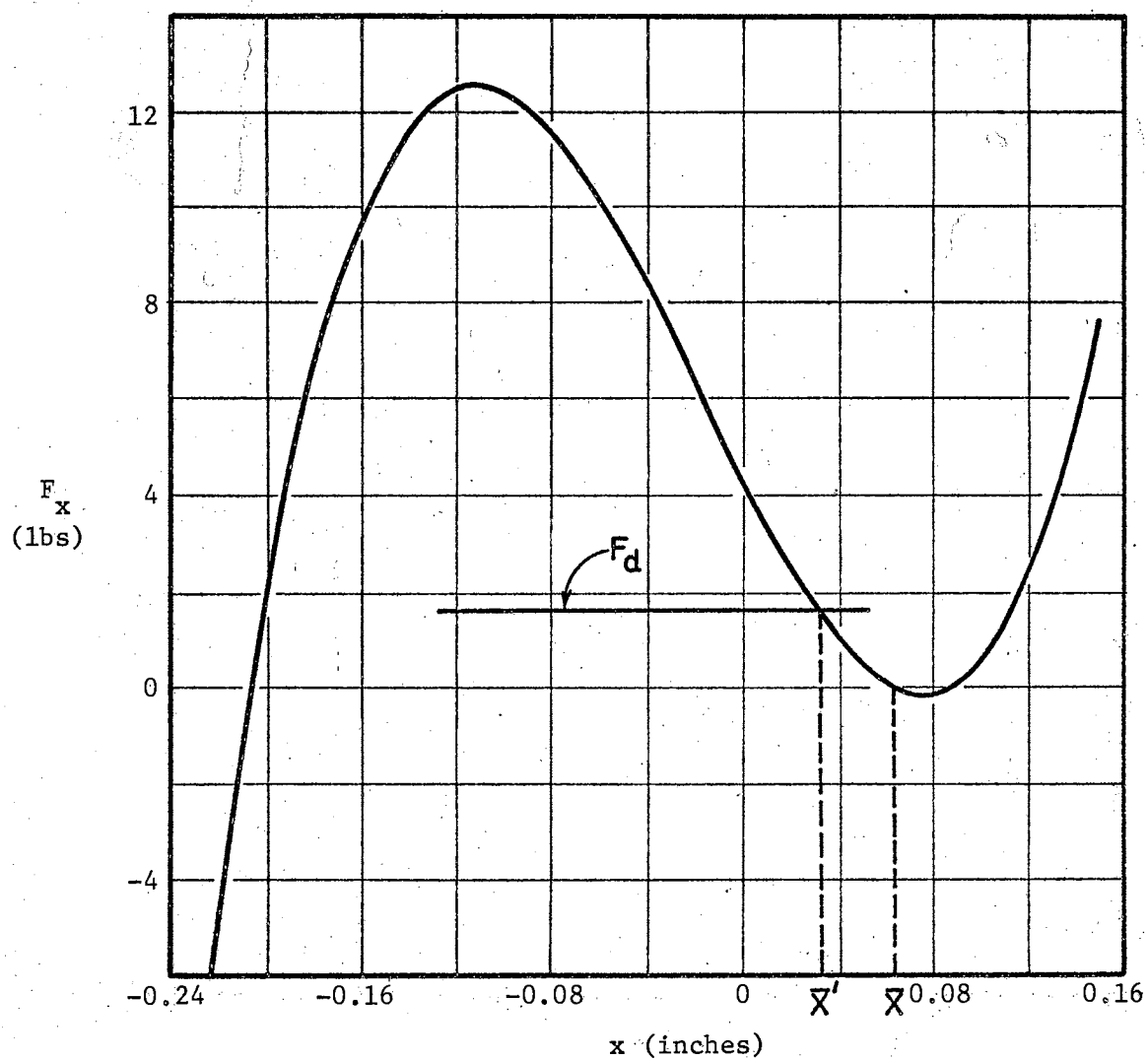


Fig. 11. Theoretical Force Between the Contacts as a Function of Displacement for  $k = 199$  lb/in,  $a = 190$  lb/in,  $m_1/m_2 = 2.815$ ,  $F_0 = 4.37$  lb and  $b = 74.54$

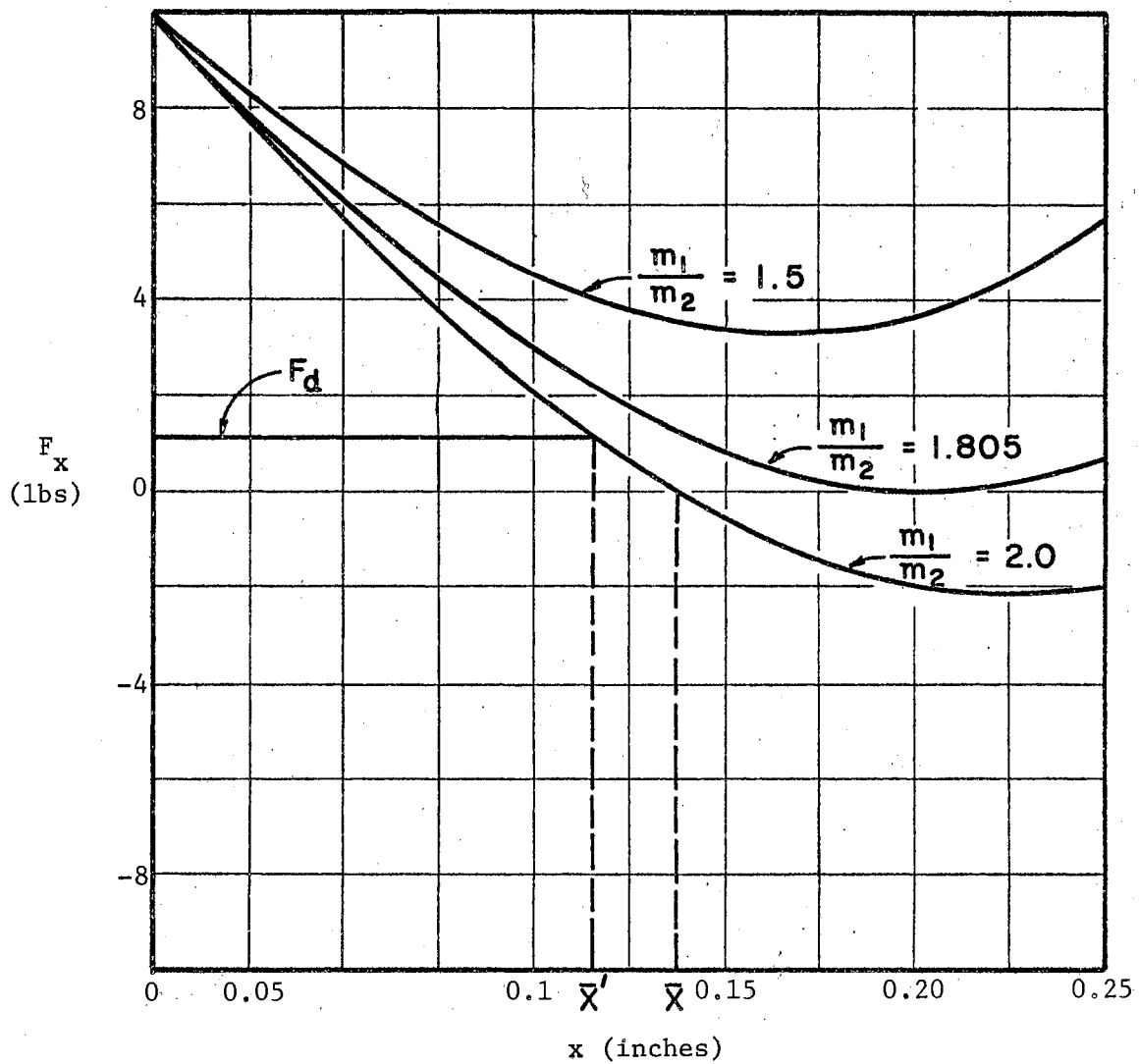


Fig. 12.  $F_x$  in the Positive Displacement Neighborhood of the Point of Vertical Tangency to the  $b = 10$  Curve of Fig. 3

of placing  $\bar{X}'$  to the left of  $\bar{X}$  for the two bottom curves. Consequently, a plot of  $\bar{X}'$  against  $\frac{m_1}{m_2}$  similar to Fig. 3 would show a contraction of the curves toward the  $\frac{m_1}{m_2}$  axis and a shift of the vertical tangencies to the left.

Figure 13 shows  $F_x$  versus displacement curves for the neighborhood of the point of vertical tangency of the  $b = 10$  curve of Fig. 7. For the preload of the number 2 curve of Fig. 13, Fig. 7 shows that separation would occur at about  $-0.4$  inches displacement. However, Fig. 13 shows that the presence of a  $0.2$  lb  $F_d$  value at  $x = 0.15$  inches would result in  $\bar{X}'$  occurring at that point. This happens to be an example of an extreme condition for the effect of differential damping on the separation criteria. The intersection of an  $F_d$  curve with curves 3 or 4 would alter the undamped separation criteria much less.

Before summarizing the effects from damping, it should be noted that the form of the damping force distribution shown in Fig. 9 is only approximately correct. However, it is the approximation which is usually accepted (11). In the case of structural damping, it is well established that above certain stress levels the damping is not linear with displacement as used here (12). With reference to Fig. 9 (a), it is seen that the deflection in each contact from the unstressed positions of  $-\delta_1$  and  $\delta_2$  is not symmetric so that the nonlinear contact is stressed higher at  $x = \beta - \alpha$  than at  $x = \alpha - \beta$  and the linear contact is stressed higher at  $x = \alpha - \beta$  than at  $x = \beta - \alpha$ . This situation indicates that the difference in the two damping forces may be expected to be greater than that shown. Also, in some cases it may be expected that there will be

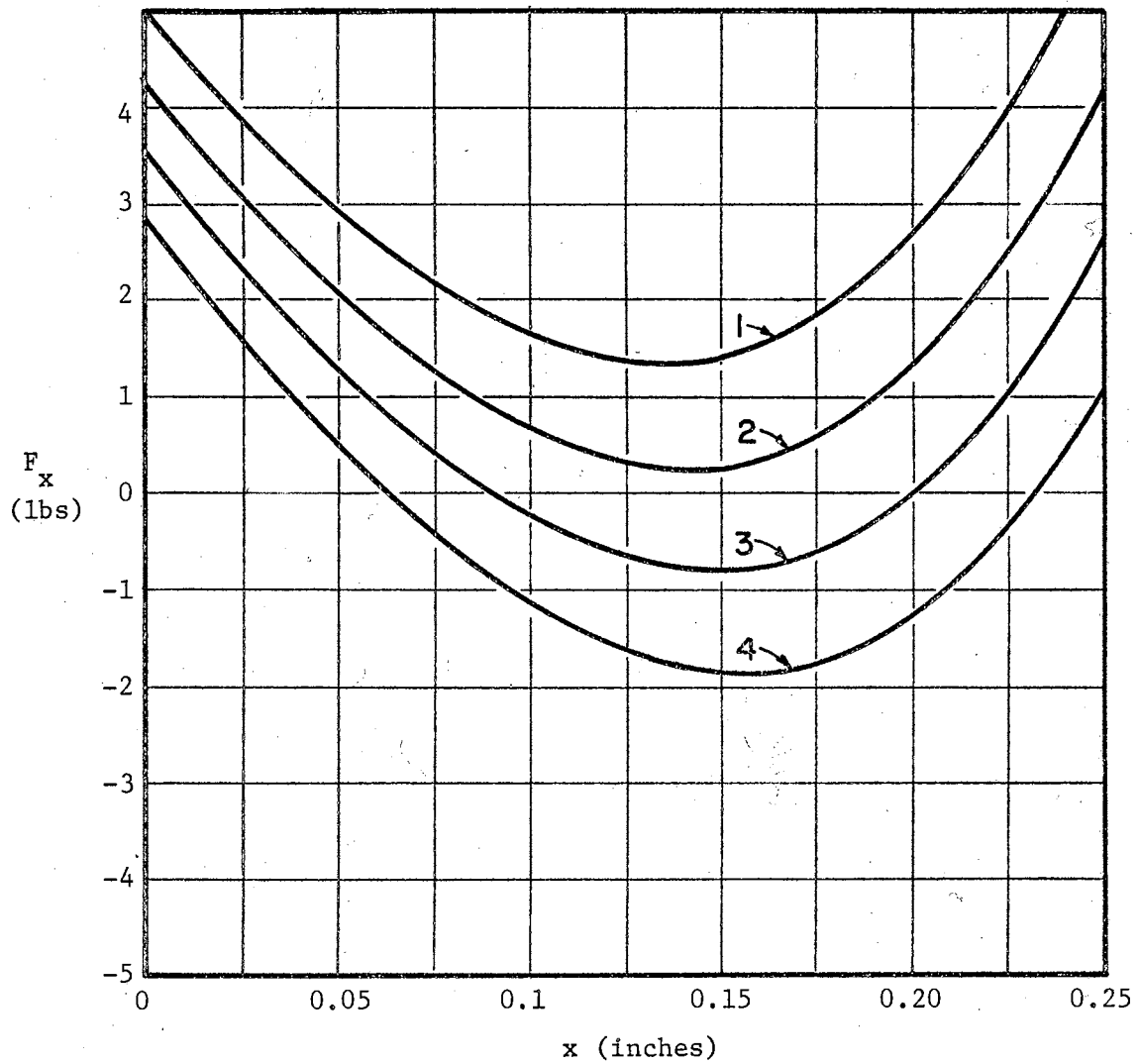


Fig. 13.  $F_x$  in the Neighborhood of the Vertical Tangency to the  $b = 10$  Curve of Fig. 7

a difference in structural damping forces when the two damping coefficients are identical.

The qualitative effect of damping on the undamped separation criteria may be summarized as follows. Damping which generates equal forces on the two contacts will not affect the criteria. The presence of different damping forces will always cause the separation displacement to be less than that predicted by the undamped criteria. The amount of difference will depend on the particular contact configuration and preload. The introduction of equal damping to limit the contact response will not materially affect the predicted separation criteria. However, it may be expected that physical limitations would prevent exactly equal damping. There also might be contact applications where damping would be detrimental from the standpoint of lengthening closing and opening times. Consequently, optimum damping may not be realizable in practice.

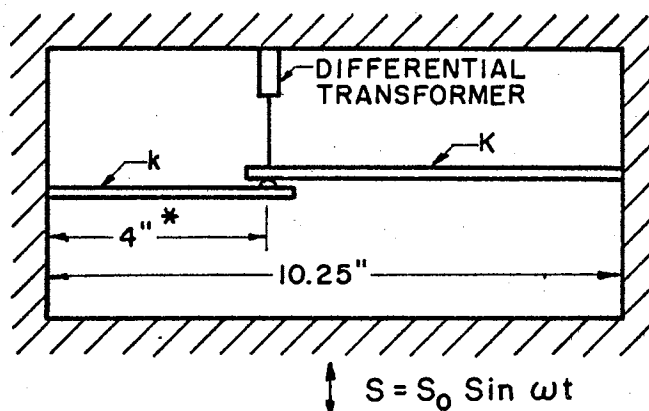
## CHAPTER IV

### EXPERIMENTAL MODEL AND INSTRUMENTATION

A large scale model of a set of contacts was constructed and instrumented so that some of the theoretical results could be tested with an electro-mechanical shaker system. The size of the model was dictated by instrumentation requirements. By making the model large, it was possible to use instrumentation which provided precise measurements without altering the characteristics of the contacts.

Several model configurations were tried, but it was found that the one described herein provided the greatest accuracy and reliability because extraneous influences and effects were minimized. In particular, damping was low and constant, and spurious resonances and harmonics were not present within the frequency range of the tests. Consequently, all reported tests were made with the described configuration.

Briefly, with reference to Fig. 14, the model and instrumentation may be described as follows. A linear cantilever beam contacted a non-linear cantilever beam through a contacting button. The preload on the contact surfaces was set by raising or lowering the linear beam. The entire system was subjected to a known sinusoidal displacement; the relative displacement of the upper contact surface with respect to the case was measured; and impending separation of the contacting surfaces was detected. A detailed description of the model and instrumentation



\* 4 in. linear beam for nonlinear investigation. Various lengths were used for linear investigation.

Fig. 14. Schematic of the Test Model

follows.

#### Description of the Model

Photographs of the model are shown in Plates I and II. Cantilever  $k$  duplicated the theoretical linear restoring element while cantilever  $K$  and the biasing cable duplicated the theoretical nonlinear restoring element. As given by Timoshenko (13), the restoring force on cantilever  $K$  from the biasing cable is approximately

$$F \approx \frac{2S}{l} y + \frac{AE}{l^3} y^3 \quad ;$$

where

$S$  is the initial tension on the cable;

$l$  is the semi-length of the cable;

$y$  is the displacement from the zero preload position;



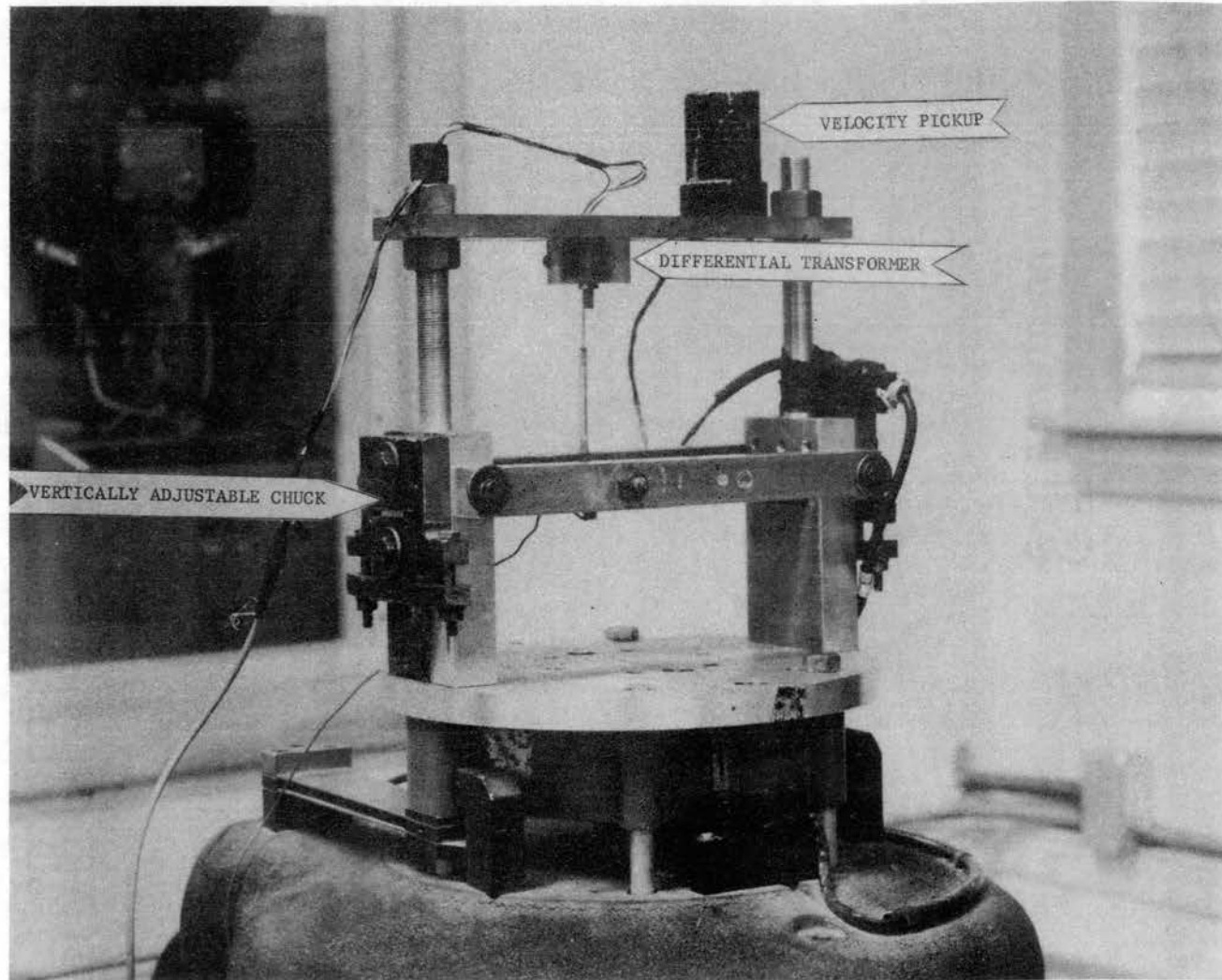


PLATE I. EXPERIMENTAL MODEL (Side View)

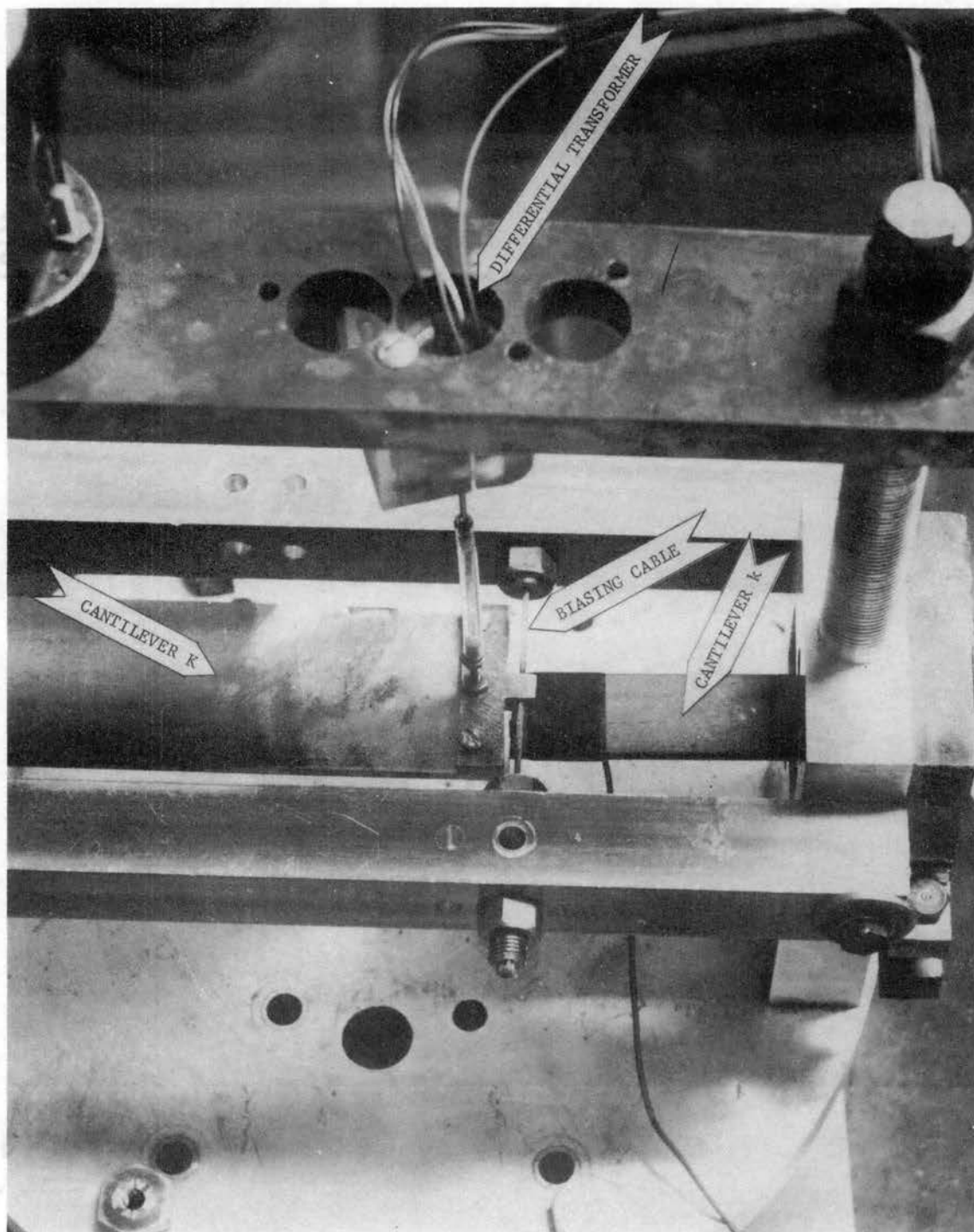


PLATE II. EXPERIMENTAL MODEL (Top View)

A is the cross sectional area of the cable material; and

E is the modulus of elasticity of the cable material.

Without the biasing cable, the system duplicated the theoretical linear case of  $b = 0$ .

The cantilever beams were made of 1/8-inch thick oil quenched 1095 steel and the biasing cable was 1/16-inch diameter 9-23 aircraft cable. Various sizes of music wire were tried as a biasing cable but were found to be so stiff in bending that failure soon occurred from excessive bending stresses. The many fine strands of the aircraft cable provided greater flexibility so that bending stresses were no problem.

The vertically adjustable chuck provided means for varying the pre-load between the contacts. The  $\frac{a}{k}$  and  $\frac{m_1}{m_2}$  ratios were varied by inserting different length cantilever beams in the chucks.

The contact surfaces were the flat bottom of cantilever K and a hemispherical steel button attached to, but electrically insulated from, cantilever k.

#### Instrumentation

A block diagram of the instrumentation is shown in Fig. 15. The impending separation of the contacts was detected by the circuitry labeled Contact Separation Detection. With a thin film of instrument oil between the contacting surfaces, a slight drop in potential across the 100,000 ohm resistor occurred as the force between the contacts approached zero. This potential drop proved to be an accurate and repeatable indication of impending contact separation. Display of the potential drop on the oscilloscope provided a visual indication of impending separation.

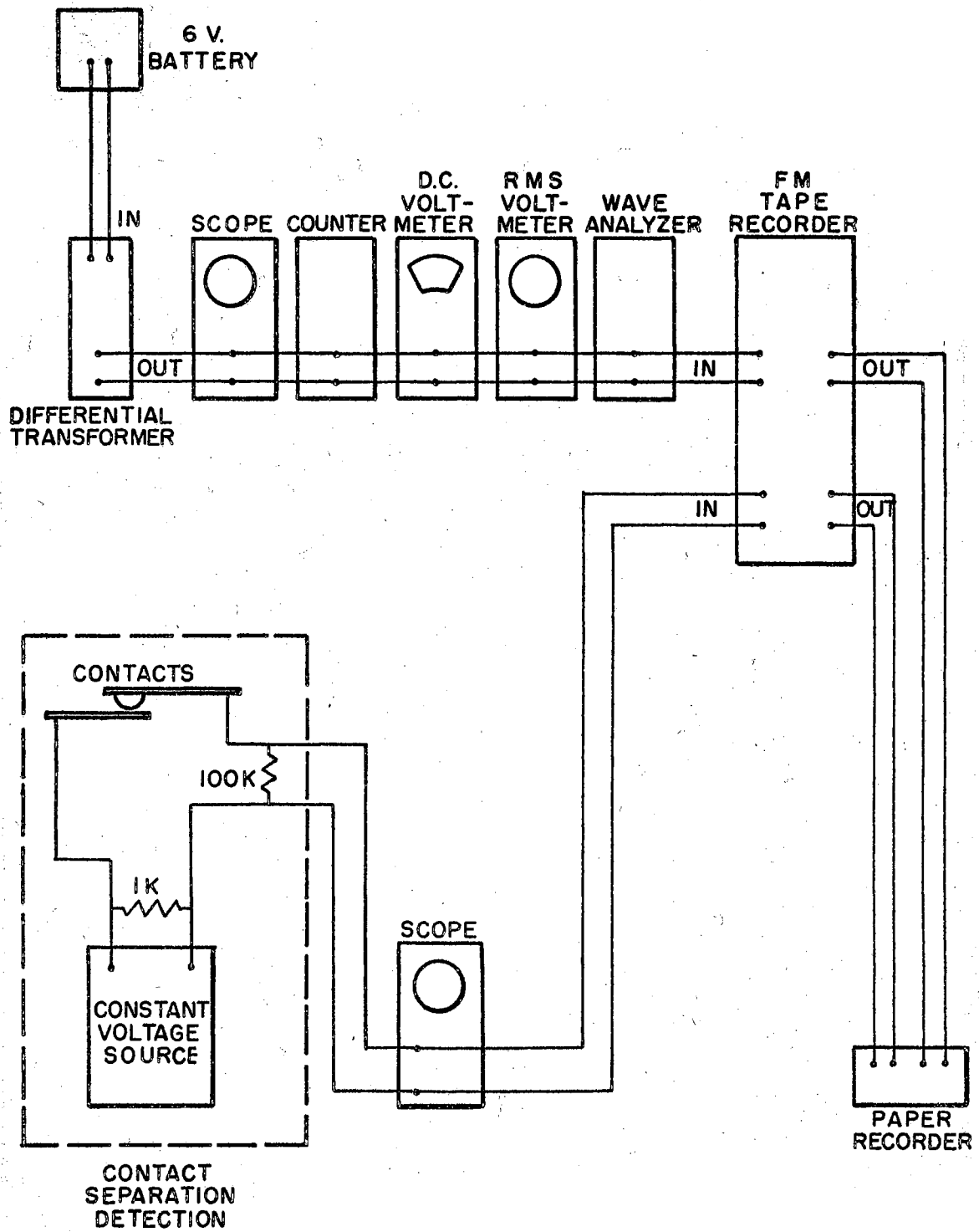


Fig. 15. Block Diagram of Instrumentation

A statically and dynamically calibrated differential transformer was used to determine the relative displacement of the contact surfaces. The entire differential transformer output was displayed on an oscilloscope. The static deflection of the contacts was measured with the D. C. Voltmeter and the sinusoidal part of the response with the RMS Voltmeter. The wave analyzer was used to measure the harmonics present in the response, and the counter measured the response frequency. The frequency modulated tape recorder provided a means of slowing down the contact response and impending separation signals by a factor of 8 so that they could be recorded on paper for further study.

## CHAPTER V

### EXPERIMENTAL PROCEDURE AND RESULTS

The model and instrumentation described in Chapter IV were used to test the theoretical separation criteria and system response for certain contact configurations and to investigate the effect on separation of the time response associated with the jump phenomenon.

The testing was first accomplished with a linear model where instrumentation reliability and data repeatability were established. This was followed with testing with the nonlinear model and investigation of the jump response. In each case the theoretical results were computed from the measured model parameters and preload for comparison with the measured values.

#### Measurement of Model Parameters and Preload

Computation of the theoretical impending separation displacement of the model required the measurement of  $a$ ,  $b$ ,  $k$ ,  $m_1$ ,  $m_2$ , and the preload.

The value of  $k$  was easily measured through use of a balance beam and dead weights for force and the differential transformer for displacement.

The ratio of the measured force to the measured displacement then gave the value of  $k$ . In the linear case, where  $b = 0$ , the same procedure provided the measured value of  $a$ .

In the nonlinear case the force versus displacement relationship was determined in the same manner. However,  $a$  and  $b$  were related through the cubic curve defined by a plot of force versus displacement points. This relationship was determined by fitting the data points to the curve  $ay + aby^3$  with the digital computer using the least squares method. The force equation resulting from this procedure for the nonlinear spring of the model with 42 data points was

$$F_K = 235(y + 74.54 y^3) \text{ lbs} \quad (19)$$

where  $y$  is measured in inches from the unstressed position of the beam and biasing cable. The values of  $a$ ,  $b$  and  $k$  were measured with the cantilevers mounted in the model so that they reflected the elasticity of the model as well as that of the cantilever beams. This provided greater accuracy because the model, although quite stiff, possessed some flexibility. The measurement of the effective masses was somewhat more complicated. Den Hartog (14) gives the approximate equivalent mass of a cantilever beam vibrating in its fundamental mode as about 23 per cent of the total mass of the beam. However, use of this value plus point masses to compensate for the attachments to the beam gave poor results. This was primarily because there is no such thing as a perfectly built-in beam as reflected in the cantilever theory.

Because of these difficulties the effective mass was determined by an indirect method. The natural frequencies of the beams were measured and the effective masses determined from the relation

$$m = \frac{k}{(2\pi f)^2} \quad ,$$

where  $k$  is the spring constant and  $f$  is the natural frequency. For the nonlinear beam the natural frequency was measured at very low amplitude so that it would approximate the natural frequency with  $b = 0$ .

The preload was determined in each case by measuring the deflection  $\delta_1$  in the cantilever  $K$  and computing the force which gave the deflection. With the differential transformer nulled at the zero preload position, the D. C. Voltmeter of Fig. 15 indicated the preload deflection in the beam.

#### Measurement of Impending Separation Displacement

The response of the contacts relative to the model was measured with the differential transformer. With reference to Equation (17), the  $\alpha$  value was indicated by the D. C. Voltmeter and the RMS value of  $\beta$  by the RMS Voltmeter. In the linear case there was no biasing of the response so the DC component was zero. In the nonlinear case the biasing was negative and increased in absolute magnitude with response amplitude as predicted theoretically.

The differential transformer was rated as flat within 3 db for an amplitude of 0.05 inches for 0-350 cps with a 6 vdc excitation. To provide greater accuracy of measurement, the transformer was calibrated statically and over the frequency range of use. This calibration was then used in converting the electrical readings to displacement values. The readings were also corrected for any change of exciting DC voltage.

The differential transformer readings were taken by holding exciting frequency constant and slowly increasing exciting amplitude until impending separation was detected.



Since all measured impending separation occurred at a positive displacement value, the amount of nonlinear biasing in the response was subtracted from the response amplitude. In other words, the measured impending separation displacement was equal to  $\beta - \alpha$  of Equation (17).

### Experimental Results

Tests were made to check the theoretical prediction that the displacement for impending separation was independent of the frequency at which the contacts were excited. The results of three such tests are shown in Figs. 16, 17, and 18. The first two show the results for the same linear configuration but with different preloads. Figure 20 shows the results for the nonlinear configuration with one preload. Similar results were observed for other preloads and configurations.

The natural frequency of the preloaded contacts was 126.4 cps for the linear configuration of Figs. 16 and 17. The lowest and highest frequency of recorded data indicates the minimum and maximum frequencies for which impending separation could be obtained with a 20 g excitation of the model. The natural frequency for very small amplitude of the nonlinear configuration was 104.6 cps.

The data point scatter for the three figures is not excessive when instrument readability is considered. The results substantiate the theoretical prediction that the separation displacement is a function of system parameters and preload, and is independent of the exciting frequency.

Tests were also conducted to determine the effect of varying preload on the separation displacement. The results of two linear tests are

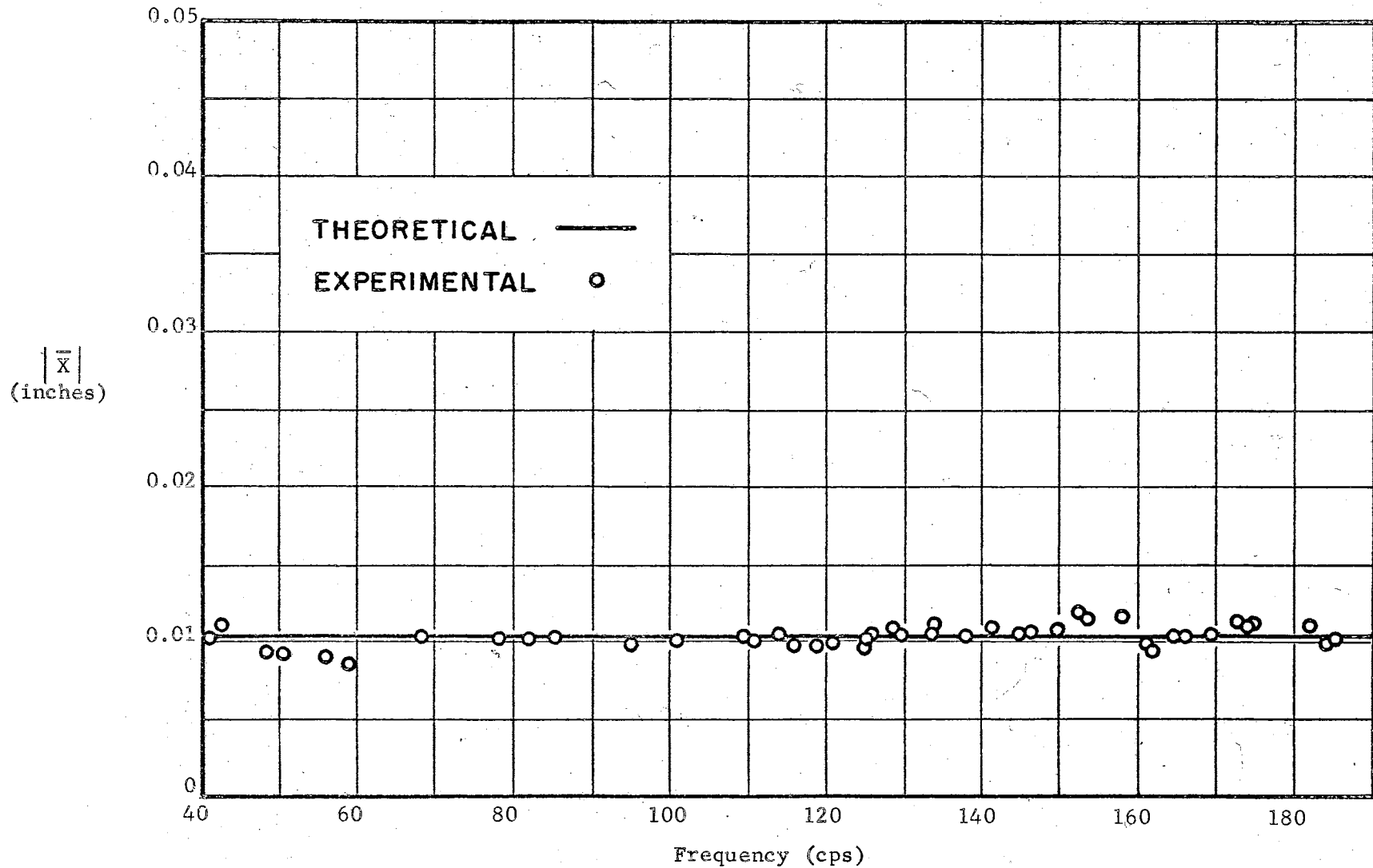


Fig. 16. Theoretical and Experimental Displacement for Impending Separation for Varying  
 Exciting Frequency,  $k/a = 3.67$ ,  $m_1/m_2 = 1.157$ ,  $b = 0$  and  $F_0 = 1.56$  lb

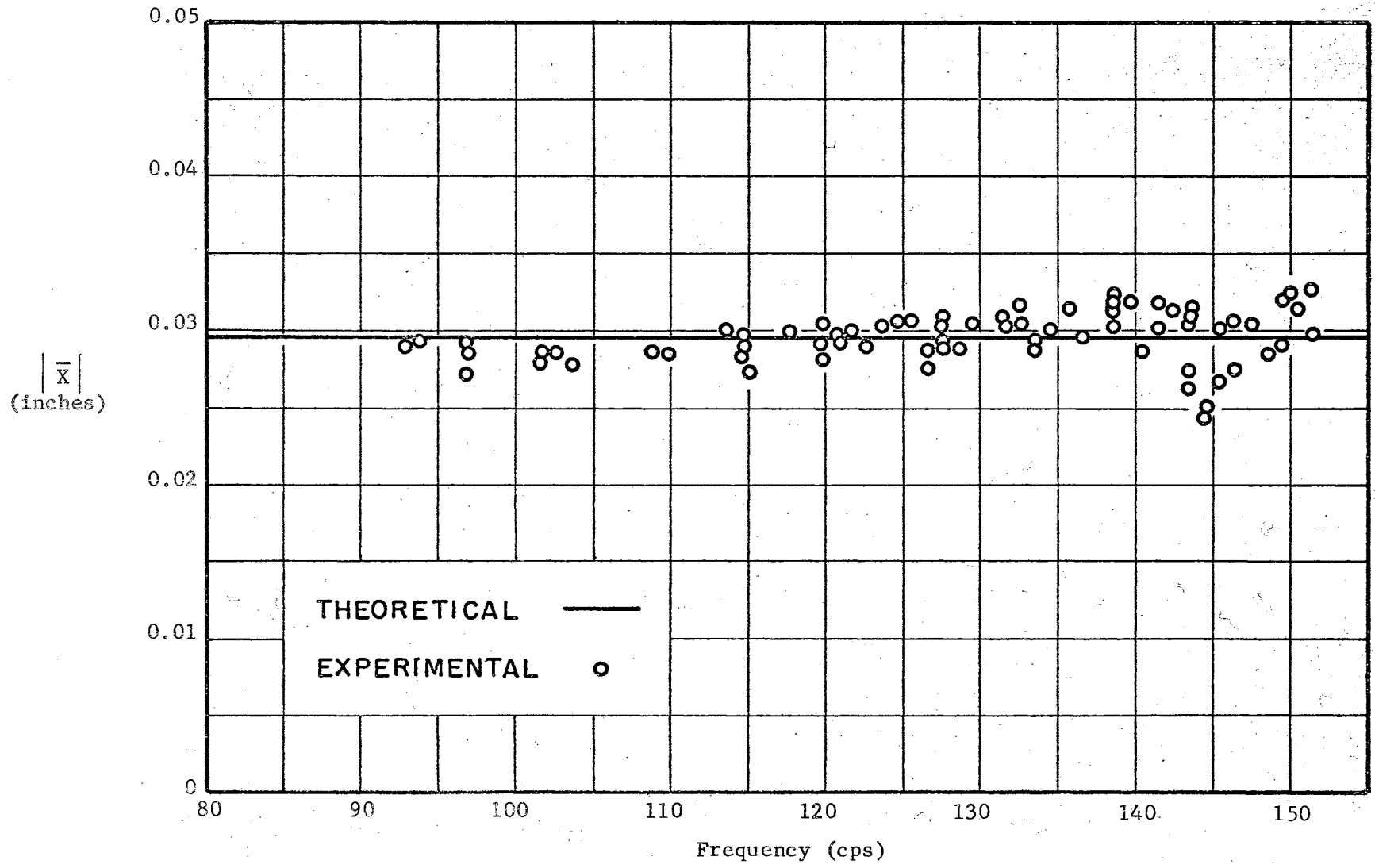


Fig. 17. Theoretical and Experimental Displacement for Impending Separation for Varying Exciting Frequency,  $k/a = 3.67$ ,  $m_1/m_2 = 1.157$ ,  $b = 0$  and  $F_0 = 4.43$  lb

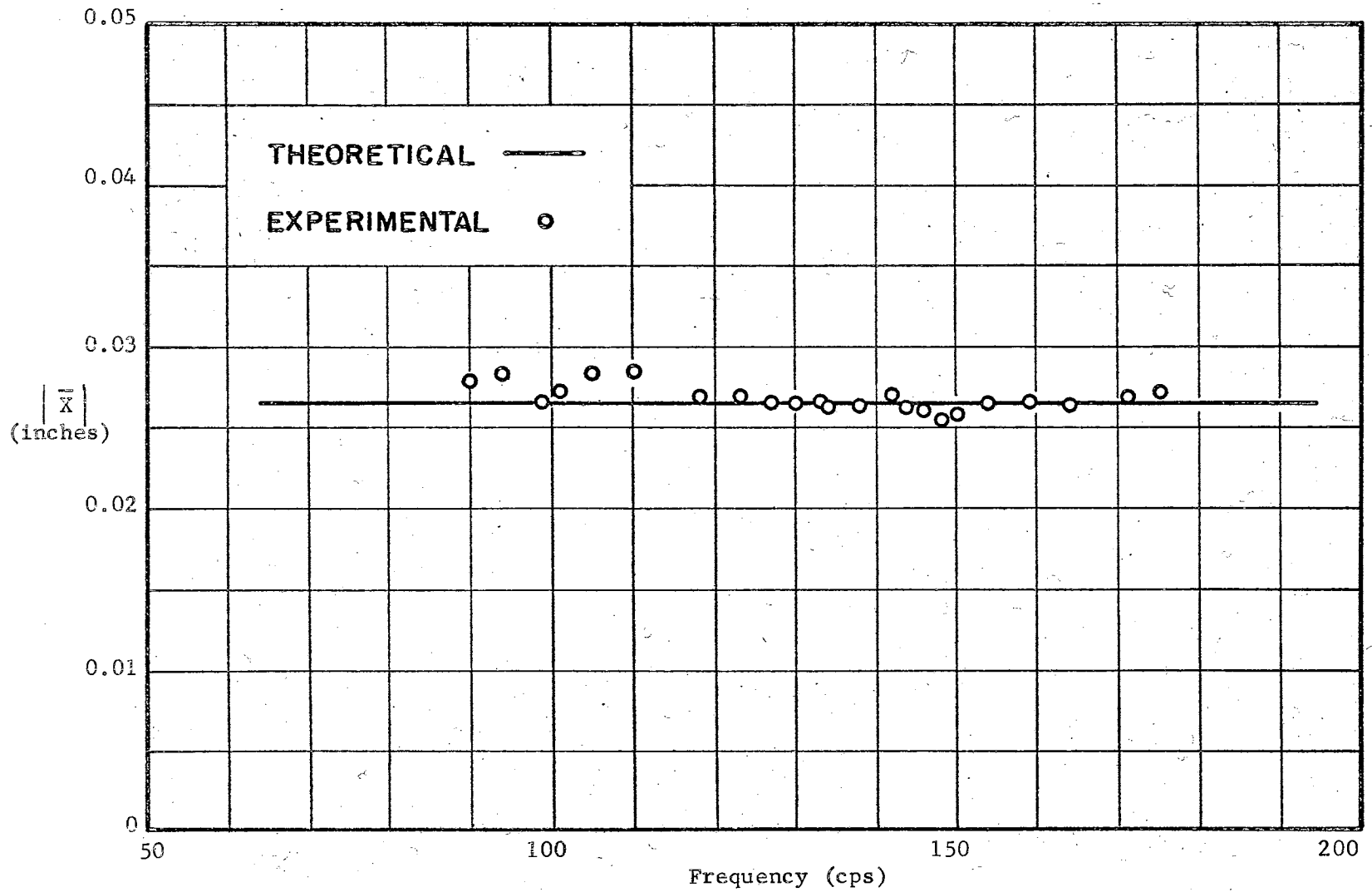


Fig. 18. Theoretical and Experimental Displacement for Impending Separation for Varying<sup>-2</sup> Exciting Frequency,  $k = 199$  lb/in,  $a = 235$  lb/in,  $m_1/m_2 = 2.815$ ,  $b = 74.54$  in and  $F_0 = 2.52$  lb

shown in Fig. 19. The data points of the upper curve come closer to coinciding with the theoretical values than those of the lower curve. This may have been due to less accurate measurement of the lower curve system parameters. In any case, both sets of data support the linear relationship between preload and the separation displacement.

The results of varying preload with the nonlinear configuration are shown in Fig. 20. Attempts were made to obtain data with higher preloads than those shown. However, yielding of the biasing cable anchors was associated with these attempts so that no reliable data could be obtained. Resetting the biasing cable tension after yielding approximately restored the force-displacement relationship of Equation (19) so that the data points shown were repeatable.

Figure 21 shows the measured values of  $\delta_1$ ,  $\delta_2$ , and  $\alpha$  corresponding to the experimental preloads of Fig. 20. The scatter of the  $\alpha$  points is attributed mainly to the readability of the D. C. Voltmeter. Even with the scatter, the trend of  $\alpha$  with increasing response amplitude of the contacts is established. The trend of  $\delta_1$  with increasing preload indicates the stiffening of the nonlinear contact with deflection. However, the stiffening is not as pronounced as might be expected from a cursory examination of Equation (19). The small magnitude of the deflections results in a small effect from the  $y^3$  term.

Figure 22 shows theoretical  $F_x$  versus displacement curves for the preloads corresponding to data points 1, 2 and 3 of Fig. 20. The experimental points of zero force between the contacts are indicated on the curves. These points indicate the size of differential damping forces

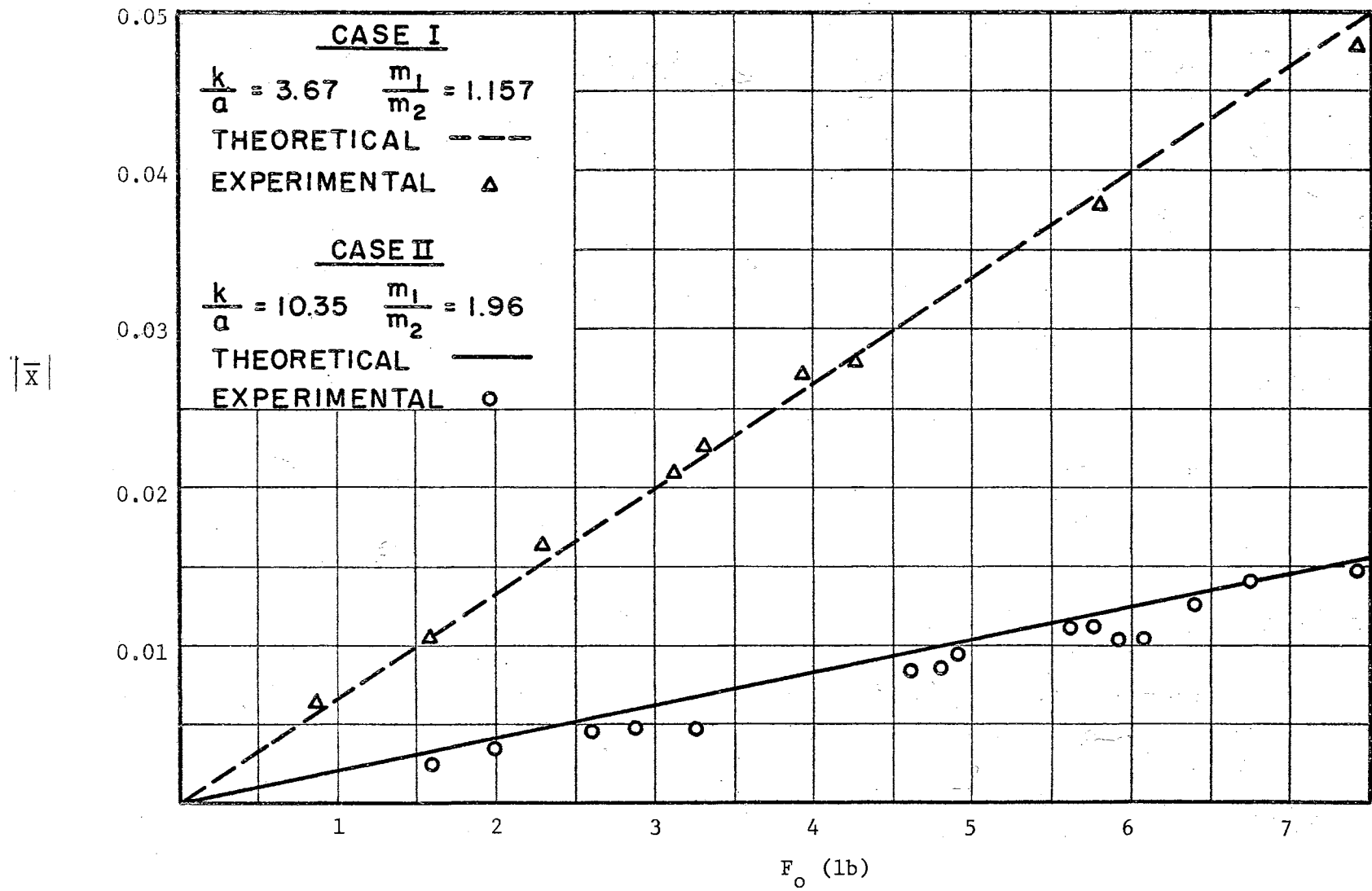


Fig. 19. Linear Theoretical and Experimental Relative Displacement for Separation as a Function of Preload

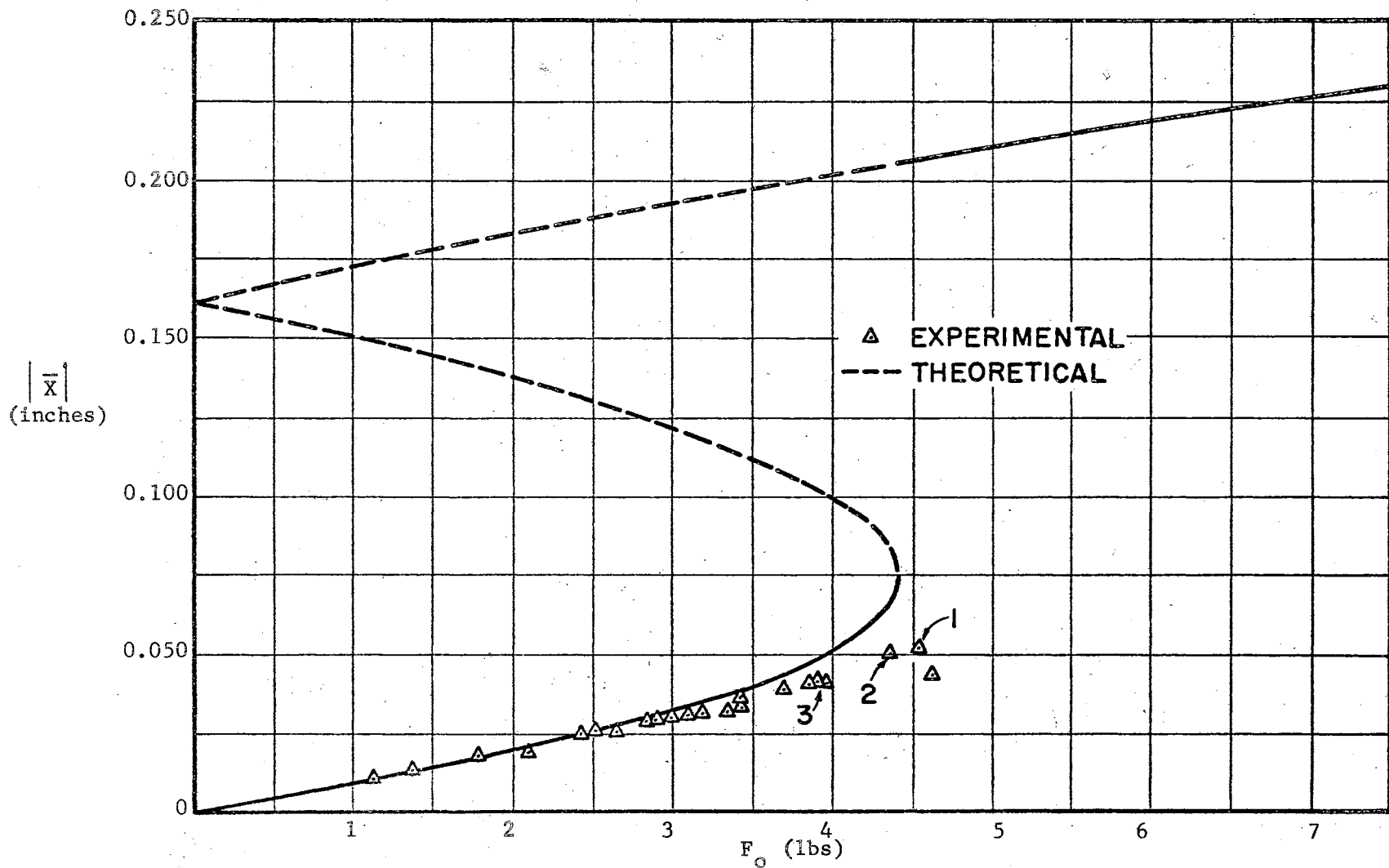


Fig. 20. Theoretical and Experimental Separation Displacement as a Function of Preload,  
 $m_1/m_2 = 2.815$ ,  $k = 199$  lb/in,  $a = 235$  lb/in,  $b = 74.54/\text{in}^2$

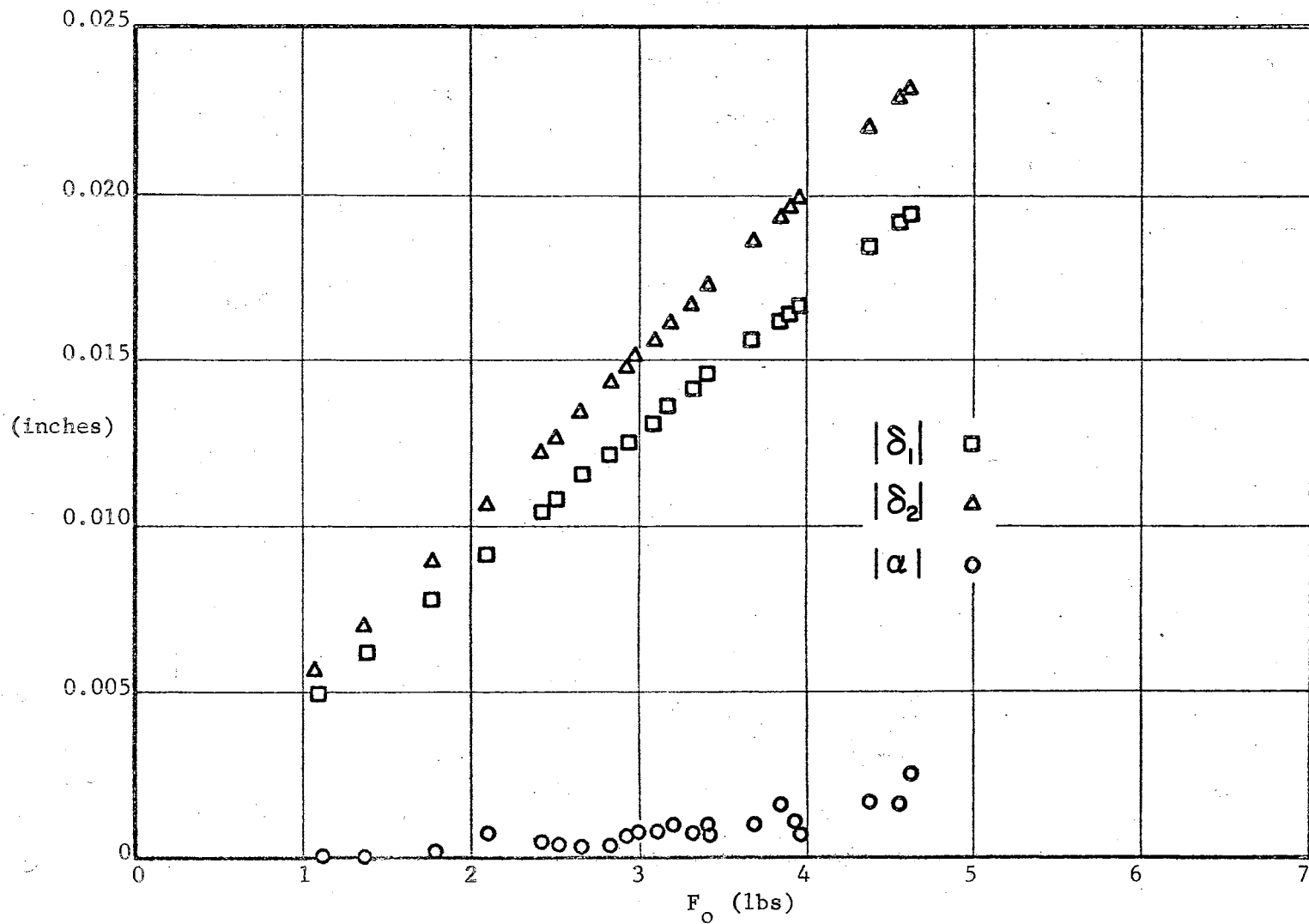


Fig. 21. Experimental  $\delta_1$ ,  $\delta_2$ , and  $\alpha$



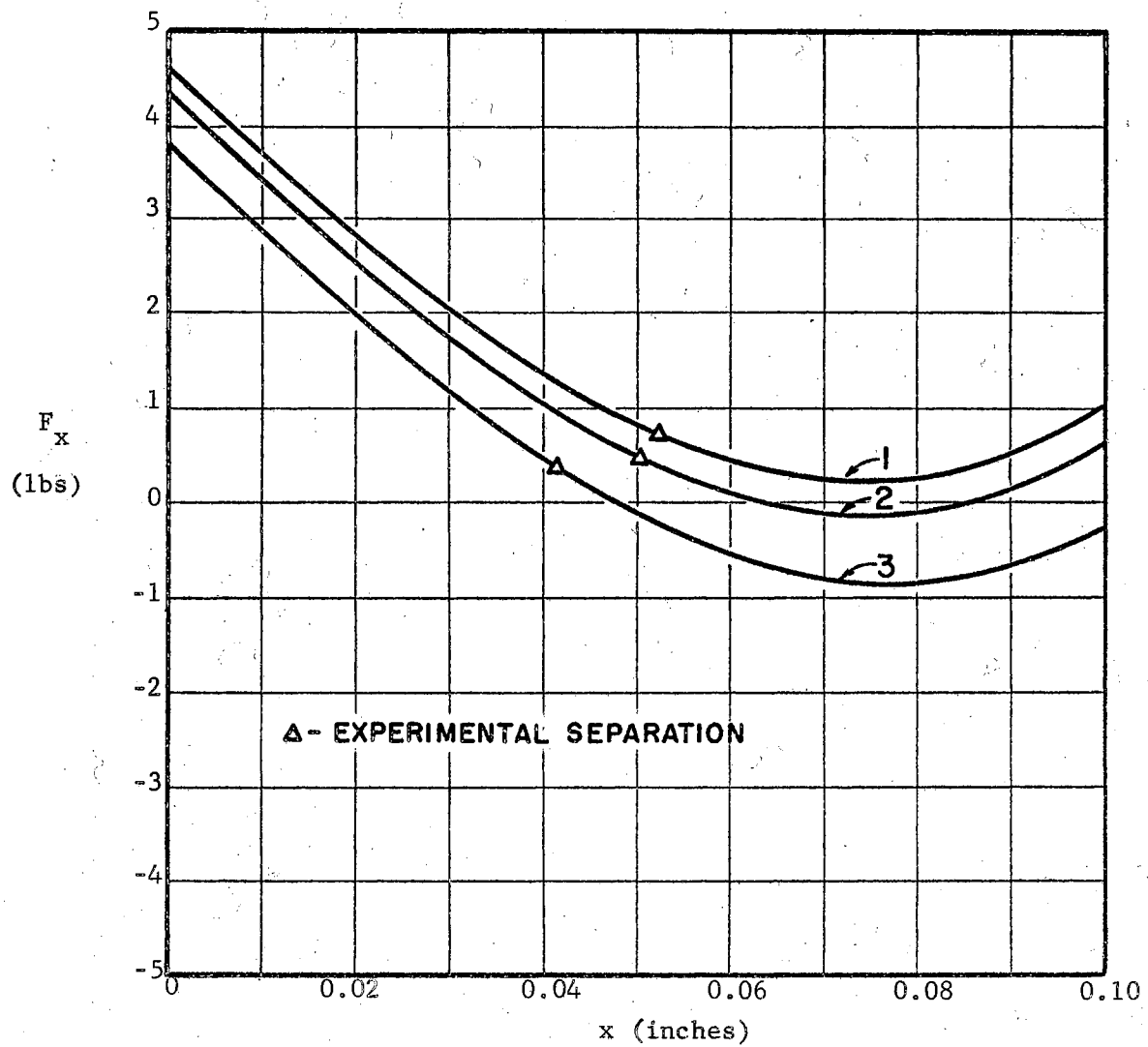


Fig. 22. Theoretical Force Between the Contacts and Experimental Points Where the Force Became Zero

which would have had to be present to account for the difference between the theoretically predicted separation displacement and that actually measured provided differential damping were the sole cause of the difference. In each case, a differential damping force of less than one pound would account for the experimental separation. Although the complexity of the biasing cable system might be expected to increase friction damping considerably with increasing preload and response amplitude, it would be presumptuous to conclude that the differences between theoretical and experimental values were solely from differential damping. Figure 23 shows a free response of the system in the time domain. From the rate of decay of the response it is evident that only small damping was associated with the contacts for the preload and response amplitude shown.

Some experimental error may be associated with Equation (19) since the measured force versus displacement was forced to fit the form of the equation. The other measurements must also have a certain amount of error associated with them, so it is remarkable, in the nonlinear case, that the theory and experiment agree as closely as they do. The theoretically predicted large jump of nonseparation displacement at the point of vertical tangency of the theoretical curve of Fig. 20 could not be tested because the yield point of the biasing cable anchors of the model would have been exceeded.

#### Effect of Nonlinear Jump Response on the Separation Criteria

The question was raised in Chapter III about the possibility that the jump response of the nonlinear configuration might cause separation

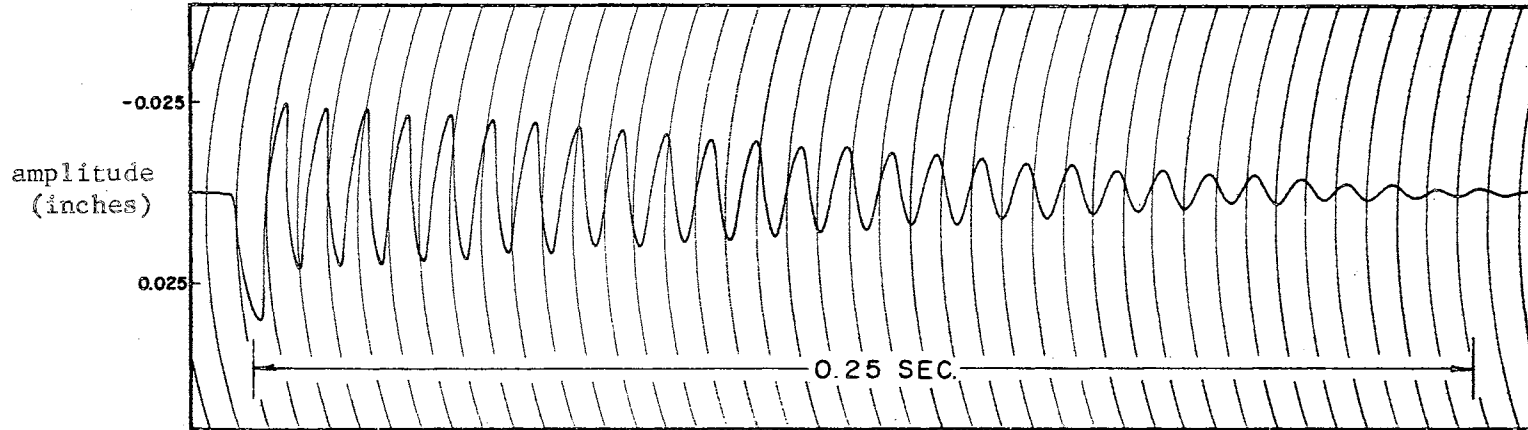


Fig. 23. Free Response of the Nonlinear Experimental System

of the contacts at some displacement less than that predicted. This possibility was investigated by varying exciting frequency, while maintaining constant exciting amplitude, until the jumps occurred. The jump response was recorded in both the frequency and time domain.

Sample jumps in the frequency domain are shown in Fig. 24. The top response is for increasing frequency and the bottom for decreasing frequency. In each case the model was excited by the displacement  $S = 0.002 \sin \omega t$  inches. The responses are outlines of oscilloscope photographs where the vertical trace was driven by the differential transformer output and the horizontal trace was driven by the frequency drive of the MB shaker system. The preload was set at about 9 lbs so that separation would not occur during the photography. The biasing of the response is evident from the figure. Comparison of the measured response with that given by Stoker (1) for a symmetric hardening system shows that the main difference is the biasing from the static equilibrium position. The up-jumps occur at a lower frequency than the down-jumps and the amplitude of jump is much greater for a down-jump than for an up-jump. It was also observed that with steady state response in the vicinity of the jump region, a small disturbance would cause the jump to take place. In all, the frequency response was precisely that given by the nonlinear theory with the single exception of the biasing. The biasing was similar to that predicted in the theory of Rauscher (6).

The response in the frequency domain provided no information about the effect of the jumps on the contact separation. However, it did tend to verify that the predicted response was obtained. It was necessary to

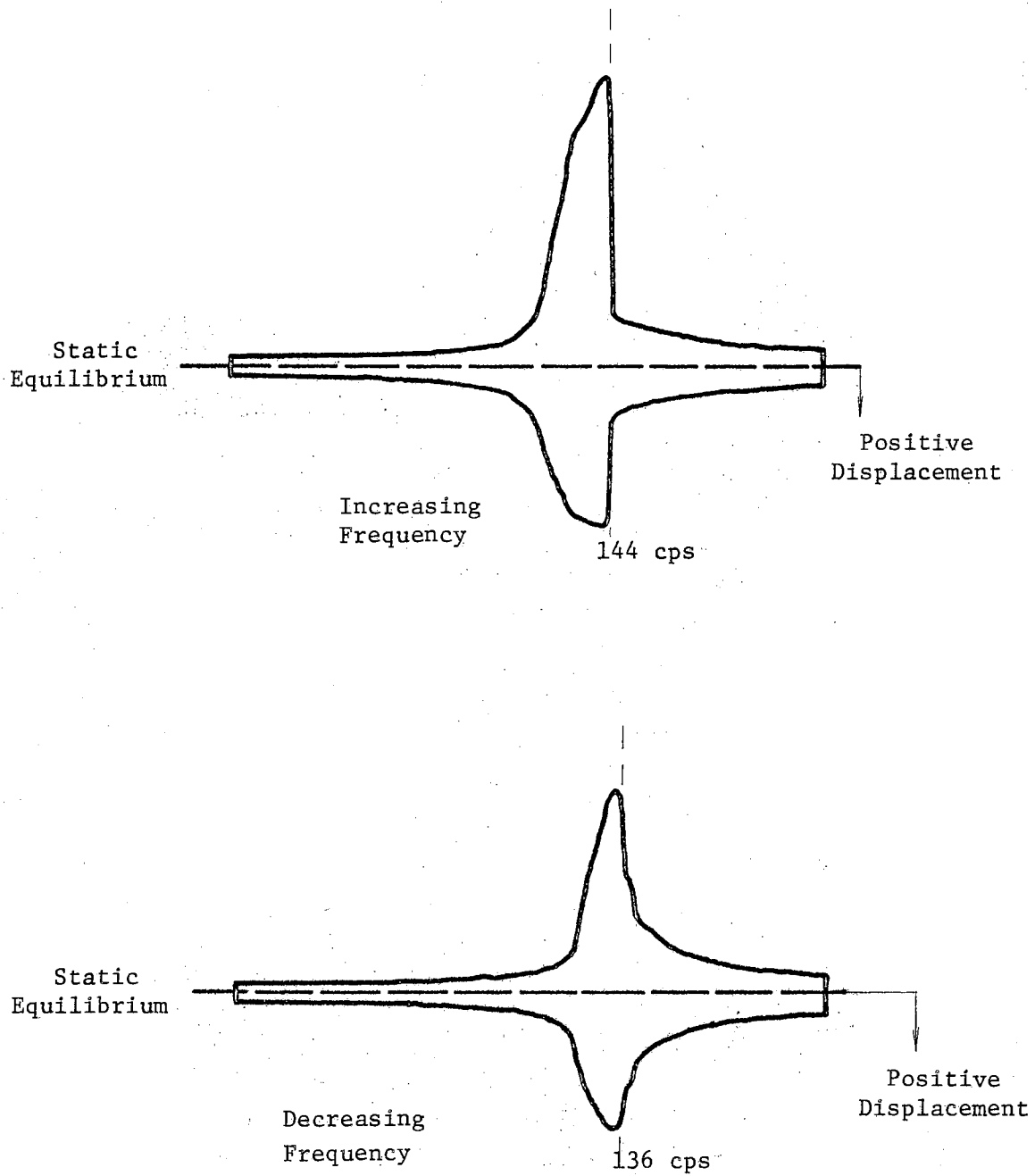


Fig. 24. Response of the Nonlinear Experimental System in the Frequency Domain.

examine the response in the time domain to determine the jump effect on separation.

As mentioned previously, there appears to be little known about the mechanism of the jump in the time domain so it was necessary to devise a means of recording the response versus time along with the detection of impending separation. This was accomplished by simultaneous recording of the differential transformer response and the separation detection signals on tape with the FM tape recorder. The frequency of response was too fast for direct recording on paper so the taped signals were slowed down by a factor of 8 and transmitted to the paper recorder. The FM circuitry permitted the time reduction without introduction of distortion. A sample recording of down-jump is shown in Fig. 25 and an up-jump in Fig. 26. Here the preload is less than that of Fig. 24 so that separation could be obtained.

Examination of Fig. 25 shows that immediately before the down-jump the contacts were separating as indicated by the signal on the top trace. During and subsequent to the jump there was no separation. After the up-jump of Fig. 26, it is seen that there is once again separation but that it ceases after six cycles. Otherwise, there is no separation. The separation from the up-jump is the result of an overshoot of the allowable displacement for nonseparation. In about thirty tests, it was found that there is no separation directly attributable to the jumps except the case of the up-jump where the overshoot goes beyond the allowable non-separation amplitude.

In Chapter III it was predicted that the time response would be essentially a biased sinusoid with little harmonic distortion. The

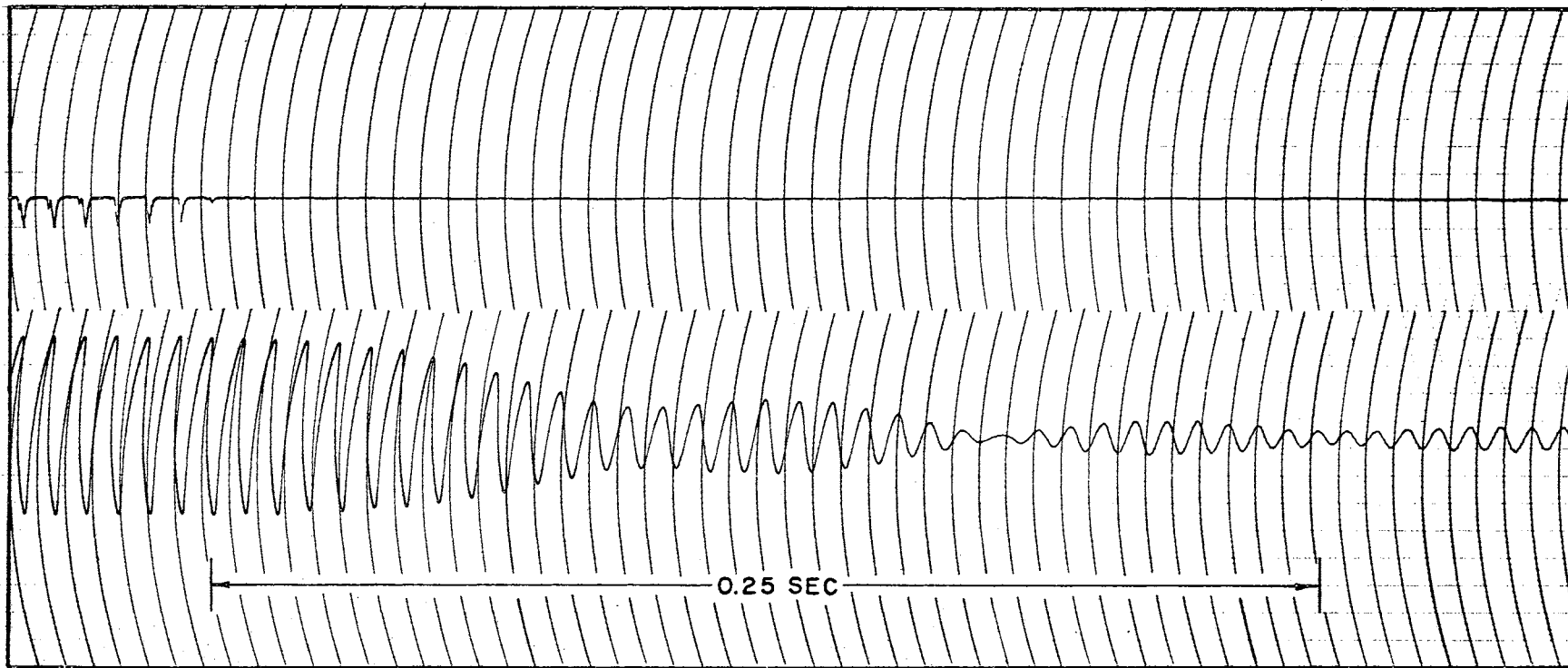


Fig. 25. Down-Jump Nonlinear Response in the Time Domain, 136 cps

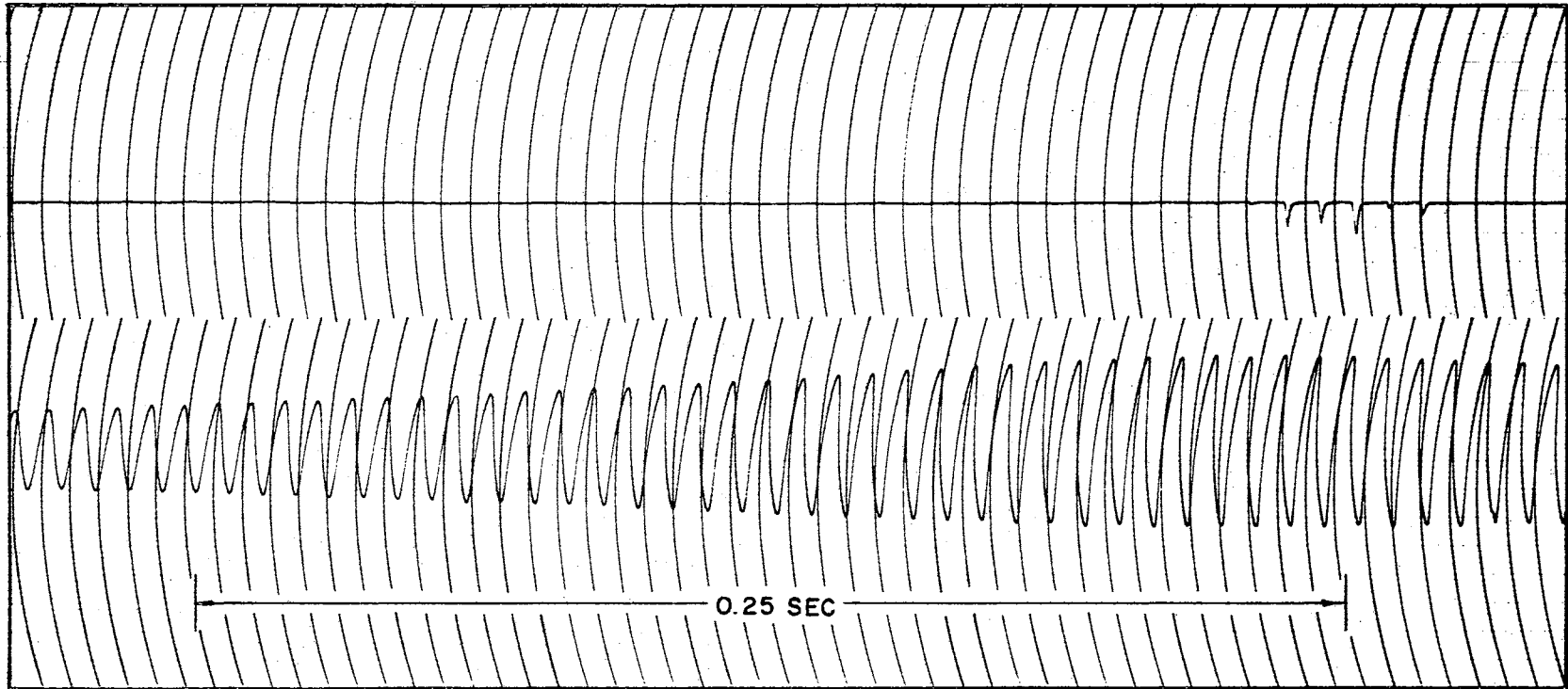


Fig. 26. Up-Jump Nonlinear Response in the Time Domain, 132 cps



observed response, other than that associated with the jumps, did not indicate the presence of harmonics which were visually recognizable. Measurements were performed with the wave analyzer to determine the exact harmonics contained in the response. It was found that four had a measurable amplitude; the second through fifth. The largest harmonic amplitudes measured were -28db (4.0 percent), -23db (7.1 percent), -38db (1.25 percent) and -40db (1.0 percent) respectively for the second, third, fourth and fifth harmonics. The measurements were with respect to the fundamental. Subharmonics were not present in the analyzed response. The presence of the even harmonics comes from the nonsymmetry of the restoring forces (5).

## CHAPTER VI

### CONCLUSIONS AND RECOMMENDATIONS

The following conclusions have been reached from the results of this study.

1. The separation criteria for a set of contacts which are subjected to a steady state sinusoidal excitation are determined solely by the contact configuration and preload.

2. The response amplitude of the contacts for nonseparation will vary from zero to large values, depending on the configuration.

3. The commonly used configuration of one rigid and one flexible contact permits no allowable nonseparation response amplitude; consequently, there is no way of preventing separation over an unlimited frequency range of excitation.

4. A linear set of contacts where each contact has the same natural frequency theoretically permits an unlimited nonseparation amplitude.

5. In many configurations, the presence of nonlinear hardening elasticity may be expected to decrease the allowable nonseparation response amplitude.

6. The separation criteria for the undamped case will hold for the damped case provided the damping generates equal damping forces on the two contacts.

7. Damping which results in unequal damping forces on the contacts will have the effect of reducing the allowable nonseparation amplitude predicted for the undamped case.

8. The only effect on the separation criteria from the nonlinear jump phenomenon is the possibility of the overshoot associated with an up-jump causing a larger response amplitude than that allowed for nonseparation.

9. The recorded jump phenomenon in the time domain could be a valuable tool in constructing an analytical solution of the jump response.

#### Recommendations for Future Study

It is recommended that further study be conducted in the area of contact response to a vibration environment. It appears that the most fruitful results will come from linear configurations. However, there may be particular situations where linear conditions will not fulfill the requirements and it would be advantageous to explore the nonlinear possibilities.

In particular, the following recommendations are made for further study with linear contact configurations.

1. That experimental work be accomplished to develop damping which will not alter the undamped separation criteria.

2. That the damping be applied to various configurations to prevent separation over an unlimited frequency range of excitation.

3. That a study be made to determine any detrimental effects from damping in the practical use of contacts in switching devices.

4. That the separation criteria be determined for shock and random excitation of the contacts.

5. That damping effects be determined for the shock and random excitation.

#### SELECTED BIBLIOGRAPHY

1. Stoker, J. J., Nonlinear Vibrations. New York: Interscience Publishers, Inc., 1950.
2. Lowery, R. L., B. C. Riddle and G. C. Stone. "Vibration Control in Relay Design," Proceedings, 11th Annual National Relay Conference 1963, Oklahoma State University, Stillwater.
3. Kubokoya, Hideo, "Dynamic Analysis of the Relay and Its Application to the Improvement of the Impulse Relay," Proceedings, 11th Annual National Relay Conference 1963, Oklahoma State University, Stillwater.
4. Takamura, M., Y. Shimizu and Y. Otuka, "Chatter Vibration of Switching Relay," Review of the Electrical Communication Laboratory, Nippon Telegraph and Telephone Public Corporation. Vol. 9, No. 3-4, March-April, 1961.
5. Duffing, G. Erzwungene Schwingungen bei veranderlicher Eigenfrequenz. Braunschweig: F. Vieweg u Sohn, 1918.
6. Rauscher, M. "Steady Oscillations of Systems with Nonlinear and Unsymmetrical Elasticity," Journal, Applied Mechanics, 5 (Trans. ASME, 60), 1938: 169-77.
7. Den Hartog, J. P., and R. M. Heiles. "Forced Vibrations in Nonlinear Systems," Journal, Applied Mechanics, 3 (1936): A-127-30.
8. Ludeke, C. A. "Experimental Investigation of Forced Oscillations in System Having Nonlinear Restoring Force," Journal, Applied Physics, 17 (1946): 603-9.
9. Dickson, L. E. Theory of Equations, John Wiley & Sons, Inc., New York, 1939.
10. Simpson, James D. "Use of the Digital Computer With the Phase-Plane Delta Method," Master of Science thesis, Oklahoma State University, Stillwater, 1963.
11. Tse, F. S., I. E. Morse and R. T. Hinkle. Mechanical Vibrations, Allyn and Bacon, Inc., Boston, 1963.
12. Dorn, John E. Mechanical Behavior of Materials at Elevated Temperatures, McGraw-Hill Book Company, Inc., New York, 1961.

13. Timoshenko, S. Vibration Problems in Engineering, D. Van Nostrand Co., Inc., New York, 1928.
14. Den Hartog, J. P. Mechanical Vibrations, McGraw-Hill, New York, 1956.

## APPENDIX A

### LIST OF SYMBOLS

a	Coefficient of the linear term of the nonlinear force versus displacement equation.
b	Ratio of the cubic coefficient to the linear coefficient of the nonlinear force versus displacement equation.
$F_k$	Restoring force exerted by the linear spring with a displacement $x$ .
$F_K$	Restoring force exerted by the nonlinear spring with a displacement $x$ .
$F_0$	Static preload on the contacts.
$F_x$	Force between the contacts as a function of the displacement measured from the static equilibrium position.
$F_d$	Differential damping force acting on the contacts.
k	Linear spring constant.
K	Designator of the nonlinear spring.
$m_1$	Equivalent mass of the nonlinear contact.
$m_2$	Equivalent mass of the linear contact
$S_0$	Amplitude of the sinusoidal excitation of the contacts.
t	Time.
x	Relative displacement of the contacts from the static equilibrium position.
$\bar{X}$	Relative displacement of the contacts from the static equilibrium position at which separation impends (undamped case).
$\bar{X}'$	Same as $\bar{X}$ but for the damped case.

- $y$  Relative displacement from the unstretched position of the nonlinear spring.
- $\alpha$  Biasing term of the contact response.
- $\beta$  Response amplitude of the contacts.
- $\delta_1$  Static deflection of the nonlinear spring from the preload.
- $\delta_2$  Static deflection of the linear spring from the preload.
- $\omega$  Circular frequency of the sinusoidal excitation of the contacts.
- $\Omega$  Circular frequency of the contact response.



APPENDIX B

LIST OF MAJOR INSTRUMENTATION

- Wave Analyzer--Model 302A; Manufacturer, Hewlett-Packard; Serial No. 018-01522.
- Universal EPUT and Timer--Model 7360; Manufacturer, Beckman-Berkley; Serial No. 1918.
- Audio Oscillator--Model 200 AB; Manufacturer, Hewlett-Packard; Serial No. 130-13888.
- FM Tape Recorder--Model 2007; Manufacturer, Sanborn-Ampex; Serial No. 244.
- Linear Differential Transformer--Model 7DCDT-050; Manufacturer, Sanborn; Serial No. FG.
- Dual Beam Oscilloscope--Model 502; Manufacturer, Tektronix; Serial No. 006852.
- Velocity Pickup--Model 4-102A; Manufacturer, CFC; Serial No. 25719.
- DC Nullvoltmeter--Model 413A; Manufacturer, Hewlett-Packard; Serial No. 139-00188.
- Vibration Test Equipment--Model T112031; Manufacturer, MB Electronics; Serial No. 121.  
Model C11; Serial No. 670.
- Vibration Meter: Model N550; Manufacturer, MB Electronics.
- Sine Random Generator: Model N670; Manufacturer, MB Electronics.
- Control Equipment: Model T251; Manufacturer, MB Electronics.
- Shaker: Model C-10; Manufacturer, MB Electronics.
- Shaker System--Model B44; Manufacturer, Calidyne.

VITA

Morris Charles Burkhart

Candidate for the Degree of

Doctor of Philosophy

Thesis: SEPARATION CRITERIA OF A NONLINEAR CONTACT SYSTEM IN A STEADY STATE SINUSOIDAL VIBRATION ENVIRONMENT

Major Field: Mechanical Engineering

Biographical:

Personal Data: Born near Pioneer, Ohio, November 12, 1923, the son of Sherman Francis and Mildred Eugenia Burkhart.

Education: Graduated from Pioneer High School, Pioneer, Ohio, 1941; received the Bachelor of Science Degree in Mechanical Engineering from Oklahoma State University in May, 1962; received the Master of Science Degree in Mechanical Engineering from Oklahoma State University in May, 1963; completed requirements for the Doctor of Philosophy Degree in January, 1965.

Professional Experience: Nineteen years as a pilot in the United States Air Force and currently performing active duty as a Lieutenant Colonel with the regular Air Force.